Received: 4 July 2023 | Accepted: 10 December 2023

DOI: 10.1111/1365-2745.14275

Journal of Ecology | BRITISH ECOLOGICAL SOCIETY

RESEARCH ARTICLE

Unravelling the biogeographic determinants of tree growth sensitivity to freeze and drought in Canada's forests

Martin P. Girardin[1,2] | Xiao Jing Guo[1] | William Marchand[3] | Claire Depardieu[1,4,5]

[1]Natural Resources Canada, Canadian Forest Service, Laurentian Forestry Centre, Quebec, Quebec, Canada

[2]Centre for Forest Research, Université du Québec à Montréal, Montreal, Quebec, Canada

[3]Institut National de l'Information Géographique et Forestière, Nogent-sur-Vernisson, France

[4]Canada Research Chair in Forest Genomics, Institute for Systems and Integrative Biology, Université Laval, Quebec, Quebec, Canada

[5]Département des sciences du bois et de la forêt, Centre for Forest Research, Université Laval, Quebec, Quebec, Canada

Correspondence
Martin P. Girardin
Email: martin.girardin@nrcan-rncan.gc.ca

Funding information
Canadian Forest Service; Natural Sciences and Engineering Research Council of Canada, Grant/Award Number: RGPIN-2019-06672

Handling Editor: Mizanur Rahman

Abstract

1. The evolutionary dynamics of tree species are influenced by their specific climatic environments, and their ability to persist is determined by adaptive strategies such as broad climate tolerance, phenotypic plasticity or genetic differentiation. Biogeographical predictions indicate that populations located at the edges of their ranges are more likely to experience heightened vulnerability to climatic fluctuations due to approaching tolerance limits. However, if local phenotypic acclimation or genetic adaptation has taken place, trees near the edge of their range could demonstrate comparable sensitivity to freeze and drought as the rest of the sampled population. Nevertheless, there remains uncertainty regarding the extent of developmental and evolutionary adjustments in climate sensitivity across the entire ranges of many tree species.
2. Here, we document the biogeography of tree growth sensitivity to freeze and soil water and vapour pressure deficits during 1950–2018 using an extensive multi-species tree-ring dataset of 35,784 trees at 4535 sites covering boreal, temperate conifer and temperate deciduous forests of Canada. We quantify the relationships between tree radial growth increment and seasonal climate variables and explore factors driving the observed patterns of annual growth and climate sensitivity such as species, regional climate and local site conditions, and tree age and size.
3. Freeze and drought had widespread impacts on tree growth that were contingent on the presence of focal species in interaction with tree size. An indirect growth thermal limitation towards cold/wet edges, occurring through the site moisture conditions, was observed in seven widespread species (e.g. *Picea glauca*, *Picea mariana* and *Larix laricina*). Moreover, six species had negative drought impacts more strongly expressed towards their warm/dry edges (e.g. *Abies balsamea*, *Betula papyrifera* and *Pseudotsuga menziesii*). However, widespread *Picea*, *Pinus* and *Populus* species showed no indication of increased sensitivity to soil water conditions at these edges.

This is an open access article under the terms of the Creative Commons Attribution License, which permits use, distribution and reproduction in any medium, provided the original work is properly cited.
© 2024 His Majesty the King in Right of Canada and The Authors. *Journal of Ecology* published by John Wiley & Sons Ltd on behalf of British Ecological Society. Reproduced with the permission of the Minister of Natural Resources Canada.

4. *Synthesis*. Our findings support the idea of evolutionary or acclimatization adjustments in the development of populations in response to long-term climate conditions experienced in their respective locations. This underscores the importance of incorporating phenotypic and genomic data into future analyses of climate change impacts, which would enhance our ability to predict potential ecological shifts.

KEYWORDS
conifers, dendrochronology, frost, hardwoods, soil moisture, tree-rings, vapour pressure deficit, water stress

1 | INTRODUCTION

Climate is known to be an important selective factor driving the divergent evolution of tree species under various growing conditions. The ability of a given tree population to persist depends on its strategy to cope with environmental development (Fei et al., 2017). At present, Canada's terrestrial ecosystems support nearly 180 tree species for which long-term selective processes limited their evolution and establishment after the last glaciation 11,500 to 8000 years ago (Dyke, 2005). The pronounced north–south temperature and distinct west–east moisture gradients, with humid coastal areas near the Atlantic and dry ones towards the interior, create uneven climatic pressures on tree species (Price et al., 2013). Furthermore, within these subcontinental climatic gradients are regional to local variations that result from the effects of lakes and elevational gradients (Cullen & Marshall, 2011; Eichenlaub, 1987). Together with fire, insects, diseases and their interactions, the climatic characteristics of the last millennia have played an important role in the formation of the country's landscape variability in terms of composition and structuring of tree species populations, rejuvenation of terrestrial ecosystems, biogeochemical cycling and maintenance of productivity (Brandt, 2009).

Climate projections for Canada indicate large increases in average annual temperatures by the end of this century due to increases in greenhouse gas in the atmosphere (Hicke et al., 2022). Greater warming is expected in winter, and in the north, although in the central regions of the continent, summer temperatures may increase as much in the south as in the north (Prairie Climate Centre, 2019; Price et al., 2013). Consequently, a drastic increase in forest mortality and poleward climate niche shifts are expected, raising serious questions about the ability of trees to evolve or acclimate and persist in the face of these rapid changes (Boisvert-Marsh et al., 2022; Hammond et al., 2022). From past selective climatic pressures, tree species have developed evolutionary patterns to acclimate and adapt to the heterogeneous environments that make up their geographic distributions (Canham et al., 2018; Leites et al., 2019). Among other things, plastic responses have been obtained by acclimation at leaf physiological and anatomical levels, for example, by controlling water loss by stomatal closure or by down-regulating respiratory rates (Reich et al., 2016; Smith & Dukes, 2013). Acclimation at the whole tree level has also been made possible by increasing the ratio of root to shoot biomass, to improve water uptake during dry periods (Bachofen et al., 2021). Such phenotypic plasticity allows rapid response to changing environmental conditions. Instead, local adaptation is a much slower process, involving several generations, leading to optimal genotypic adaptation in the local environment due to directional natural selection of tree populations (Kawecki & Ebert, 2004). This phenomenon occurred in species distributed over large and diverse areas, in the case of temporal or spatial barriers to allele exchanges between populations, and when selection was stronger than these genetic exchanges (Guo et al., 2022; Matías et al., 2014). Among other things, the long exposure of Canadian forests to xeric conditions has led to local adaptations to water stress in white spruce (*Picea glauca*) and white pine (*Pinus strobus*) populations (Depardieu et al., 2020; Housset et al., 2018). Furthermore, black spruce (*Picea mariana*) populations exposed to frost have developed strategies to delay bud burst, thereby reducing the risk of frost damage (Guo et al., 2022). Therefore, plastic responses to variable habitats as well as genetic differentiation to contrasting climates are important strategies of tree species to cope with environmental variability and climate changes (Barriopedro et al., 2011).

Although widely distributed tree species can grow in a variety of environmental conditions, for most species it is unclear whether their wide geographic distribution reflects a very wide tolerance to climatic conditions, a high degree of phenotypic plasticity or genetic differentiation (Canham et al., 2018). According to biogeographical predictions, populations located at the limits of their ranges would be more sensitive to climatic fluctuations because the conditions there approach the tolerance limits of the species (Camarero et al., 2021; Matías et al., 2017). Forests exposed to cold climatic conditions at the north edge are expected to have increased sensitivity to thermal fluctuations compared to forests in warmer environments (Babst et al., 2019). The same could be said for forests located at the rear/dry edge, where increased sensitivity to drought can be expected (Herrero et al., 2013). However, at the species level, local ecological factors, ontogeny and complex demography, or genetic adaptations may blur or override these geographic patterns of temperature and drought sensitivity (Camarero et al., 2021; Marchand et al., 2018; Vilà-Cabrera et al., 2019). The potential of trees to acclimate to climate over their lifetime via phenotypic plasticity in their functioning

is likely to also influence their sensitivity to climate (Gantois, 2022; Reich et al., 2016). For instance, trees with high phenotypic plasticity may be better able to adjust their physiological and morphological traits in response to drought conditions (Depardieu et al., 2020; Esperon-Rodriguez et al., 2020). So, to analyse the heterogeneous climatic sensitivity of species as well as the interactions with the underlying environmental gradients, it is increasingly necessary to build large ecological databases at the tree level. In this regard, large tree-ring data repositories are useful tools for investigating the climate sensitivity of tree species across sites, at an annual resolution, over long periods of time and across large spatial scales (Evans et al., 2022; Serra-Maluquer et al., 2022). Thus, tree rings provide a feasible method for testing biogeographical predictions (Charney et al., 2016; Girardin, Hogg, et al., 2016).

Here, we use a spatially extensive tree-ring dataset covering boreal, temperate conifer and temperate deciduous forests of Canada to document the biogeography of tree growth sensitivity to climate. Using mixed-effects models, we quantify the relationships between tree radial growth increment and three major seasonal climate variables driving growth of Canada's forests (Girardin, Bouriaud, et al., 2016; Girardin et al., 2022; Mirabel et al., 2023), namely the cold-season frequency of freeze days (FFD), mean summer soil moisture deficit (SMD) and mean summer vapour pressure deficit (VPD). Next, we explore factors favouring the observed patterns of annual growth and climate sensitivity such as species, regional climate and local site conditions, and tree age and size. Our null hypothesis is that climate sensitivity in trees is a random trait across species ranges, consequent of the ability of tree species to adjust their climate sensitivity to local climatic conditions via evolutionary or acclimatization adjustments (Canham et al., 2018). Our alternative hypothesis follows that of existing biogeographical predictions (Camarero et al., 2021; Matías et al., 2017; McKenney et al., 2014), whereby observed patterns of climate sensitivity are species-specific, characterized by a high degree of spatial autocorrelation, and covary with prevailing subcontinental climate gradients. Under this alternative hypothesis, we expect differing tree growth responses to FFD, SMD and VPD towards cold/wet and warm/dry edges of sampled species distributions (i.e. at the extremes or limits of the range of the species' data). This work provides context for assessments of the potential contributions of local climate conditions in shaping responses of tree populations to climate change.

2 | MATERIALS AND METHODS

2.1 | Tree-ring data

Tree-ring width measurements were obtained from CFS-TRenD v1.1 (Girardin, Guo, et al., 2021), a Canadian data repository containing increment core samples from 40,576 trees. Detailed information about acquisition and quality control of the tree-ring data used in this study were provided by Girardin, Guo, et al. (2021). Only those samples from trees greater than 30 years old were used to strike a balance between ensuring an adequate sample size and capturing the long-term growth patterns relevant to our research objectives. In total, we made use of 35,784 trees collected at 4535 sites across all of Canada's forested biomes (Figure 1a). The data represent 57 tree species, most samples belonging to boreal needleleaf species. For analyses, annual ring-width measurement series were converted into annual estimates of basal area increment (BAI, $cm^2 year^{-1}$) (Girardin, Bouriaud, et al., 2016).

2.2 | Climate data

Daily minimum and maximum temperatures (°C) and precipitation (mm) data were obtained for the period from 1950 to 2018 using the BioSIM software (Regniere & Bolstad, 1994). This software tool generates site-specific estimates of weather from Environment Canada (2013) historical observations. Weather estimation is achieved by interpolating daily data from the four closest weather stations, adjusting them for elevation and location differentials with regional gradients, and averaging values using a $1/d^2$ weight, where d is distance. In the current study, we performed interpolation of daily weather data onto a 1°×1° grid (Figure S1) and linked each tree-ring sampling site to its nearest grid point. From weather estimates, we computed the cold-season FFD at each site as the percentage of days with a minimum temperature < 0°C from November of the year prior to ring formation to April of the year contemporaneous with tree growth (i.e. the cold season; Girardin et al., 2022). We also computed daily VPD (in KPa), the difference between actual atmospheric water vapour amount and the maximum amount at saturation for a given temperature. A high VPD indicates that the air is dry, while a low VPD indicates that the air is close to being saturated with water vapour. Next, we calculated the soil moisture index (SMI, expressed as relative % water content), using a quadratic-plus-linear formulation procedure based on water lost by evapotranspiration and gained from precipitation (Girardin, Guo, et al., 2021; Hogg et al., 2013). We converted SMI into a SMD index:

$$SMD_{hT} = -SMI_{hT}, \quad (1)$$

where h represents the site and T represents the year. This transformation was useful for comparing the direction and magnitude of the soil moisture's effect on BAI with the other predictors. A SMD value of −100% means soil moisture is at saturation while a value of 0% means soil moisture is at the wilting point. Summer means (June to August) of daily VPD and SMD were computed.

The mean climatologies were characterized by mean annual temperature (MAT, °C) and mean annual total precipitation (MAP, mm), calculated annually from 1951 to 2018 and averaged across all years (Figure 1b,c). MAT varies widely, with the warmest climates (>5°C) mainly along the southern border and the Pacific coastline, while the coldest MAT values (<−5°C) occur in northern Canada, especially the Arctic regions. MAP shows significant spatial variations, with the west coast receiving ample precipitation (>1500 mm), central and northern regions receiving comparatively less (<400 mm), and

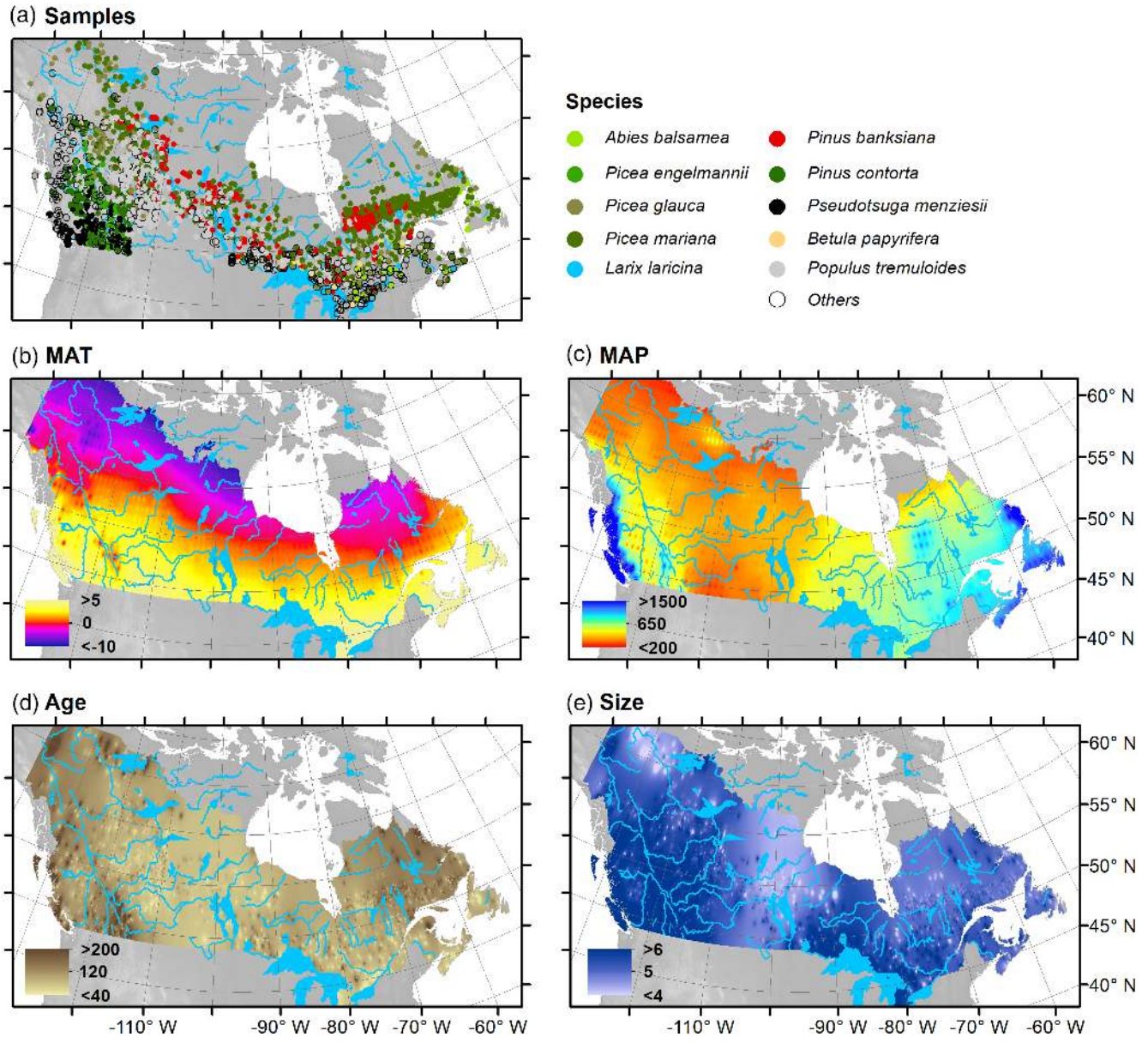


FIGURE 1 Geographical distribution of the studied tree species and the predictive variables used in the analysis of growth sensitivity to climate. (a) Sample distribution of the most widespread sampled species ($N > 100$ sites) is represented by coloured circles, while other species are shown using empty circles. Spatial distribution of the mean annual temperature (MAT, in °C; (b)) and the mean annual precipitation totals (MAP, in mm; (c)) is illustrated for the 1951–2018 period. (d and e) Mean age of tree samples (years) and mean basal area of tree samples (basal area (BA), in log mm^2). Data for tree age and BA were interpolated by applying an Inverse Distance Weighted method to the vector of georeferenced data (sampling for interpolation was set at $n = 100$ trees with a search radius of 10 degrees and resolution of 0.1 degree; ArcGIS v10.5.1).

eastern Canada, including the Maritimes, receiving an intermediate amount (600–1500 mm).

2.3 | Statistical analyses

2.3.1 | Annual growth and climate sensitivity

We used generalized additive mixed models (GAMM; Wood, 2003) to explore the effect of climate on tree growth. To do this, we modelled BAI as a function of tree ontogeny (cambial age and tree size), and the explanatory climate variable FFD, SMD and VPD, and prior-year SMD and VPD (denoted here as $SMD_{(T-1)}$ and $VPD_{(T-1)}$), so to account for carbohydrate reserve mobilization and dynamics (Richardson et al., 2013). Tree size is herein represented by inner bark basal area (BA), that is, the sum of BAI from innermost to outermost rings (cm^2). A logarithmic-power transformation (log) was applied to BAI and BA because of the skewed distributions of their values. We then fitted GAMMs per species site on each climate variable that took on the form:

$$\begin{aligned}\log BAI_{hkp.T} &= \beta_{0hp}\log\left(BA_{hkp.T-1}\right)+s_{hp}\left(cambial\ age_{hkp.T}\right)\\&+\beta_{chkp}clim_{ch.T}+Z_{hkp}B_{hkp}+\nu_{hkp}+\varepsilon_{hkp.T},\end{aligned}\tag{2}$$

where h represents the site, k represents the tree, p represents the species, c represents the climate variable, T represents the year, and the ε residual error. Cambial age refers to an estimation of tree age based on the ring counts (age). We explored the climate effects at the level of individual trees by setting tree identity as categorical variable in the model (β_{chkp}). Examining the impacts at the individual tree level enables us to capture the intra-site variability that can be associated with the age or size of trees within heterogeneous stands. We considered tree identity ($Z_{hkp}B_{hkp}$) as a random effect and included the first-order autoregressive (AR1) correlation structure (ν_{hkp}) in the model. The smoothing term, s, represents a cubic regression spline for which the degree of smoothness was determined through an iterative fitting process (Wood, 2003). Parameters for spline fitting and numbers and placement of knots were left to default values. We used the t statistics of the parameter estimates to report on the growth sensitivity to climate variables (t_{FFD}, $t_{SMD(T-1)}$, $t_{VPD(T-1)}$, $t_{SMD(T)}$, $t_{VPD(T)}$) and their associated p-values for the level of significance. The null hypothesis 'no climate effect on growth' is rejected when the p-value is lower than 0.050. The GAMMs were fitted using the 'mgcv' package version 1.8-4 (Wood, 2017) in R (R Development Core Team, 2022).

2.3.2 | Factors modulating annual growth and climate sensitivity

We examined the local spatial structure of t_{FFD}, $t_{SMD(T-1)}$, $t_{VPD(T-1)}$, $t_{SMD(T)}$ and $t_{VPD(T)}$ by using Moran's I spatial correlograms ('spdep' R package v1.1-5; Bivand & Wong, 2018). Moran's I correlograms measure spatial autocorrelation of climate sensitivity values based on site locations. The p-value is provided to evaluate the significance of that index. One seeks to reject the hypothesis of a random spatial distribution of climate sensitivity t when the corresponding p-value is lower than 0.050.

We proceeded as described below to gain insight into the potential factors driving growth sensitivity to climate. We examined the effects of species, mean climatologies and elevation at each site, and tree ontogeny, on t_{FFD}, $t_{SMD(T-1)}$, $t_{VPD(T-1)}$, $t_{SMD(T)}$ and $t_{VPD(T)}$, using a generalized additive model (GAM). Variables characterizing tree ontogeny included tree age (years) and size (logBA) at the time of sampling (Figure 1d,e). In the first stage, we fitted five models separately that took the following form:

$$\begin{aligned}t_{chkp} &= \sum_{i=1}^{N_c} s_{ci}^{(1)}\left(\overline{clim}_{ih}\right)+\sum_{i=1}^{N_o} s_{ci}^{(2)}\left(ontogeny_{ihk}\right)\\&+s_c^{(3)}\left(elevation_h\right)+s_c^{(4)}(spatial)+s_c^{(5)}\left(Z_hB_h\right)\\&+s_c^{(6)}\left(Z_pB_p\right)+\varepsilon_{chkp},\end{aligned}\tag{3}$$

where t_{chkp} represents the t statistics from equation 2 (t_{FFD}, $t_{SMD(T-1)}$, $t_{VPD(T-1)}$, $t_{SMD(T)}$ and $t_{VPD(T)}$), at site h, for tree k, and species p. $\overline{clim}_{ih}$ represents the mean MAT and MAP ($Nc=2$) for site h, and $ontogeny_{ihk}$ represents age and size ($No=2$) for site h and tree k. This multi-species model was built using all trees of which the species have 20+ sites and 100+ trees to ensure sufficient spatial variability. The three leftmost parts are additive sums of smooth functions (s) of covariates. The term *spatial* explicitly models the joint effects of latitude and longitude to capture the spatial dependence. Site identity, Z_hB_h, and species, Z_pB_p are accounting for the site and species random effects accordingly. The 'bam' function was used for estimation and the associated fast restricted maximum likelihood REML (fREML) method to fit the model (Reiss & Ogden, 2009; Wood, 2011). We used cubic regression splines as smooth functions for the climate, ontogeny and elevation (knot value $k=5$ to avoid over wiggly fitting). We also included isotropic smooths on the sphere for modelling of the spatial effects (with longitude and latitude as arguments, and basis dimension $k=500$). Residuals were tested for the presence of spatial dependencies using Moran's I described above. The strength and significance of smoothed terms were assessed using the associated F-ratio and p-value. The null hypothesis of the test states that the processes promoting the observed pattern of annual growth and climate sensitivity are unrelated to covariates MAT, MAP, Age, BA, elevation and spatial effects. This null hypothesis is rejected when $p<0.050$. The GAM models were fitted using the 'mgcv' package v1.8-33 (Wood, 2017) in R v4.0.4 (R Development Core Team, 2022) on the Narval cluster of the Digital Research Alliance of Canada (https://alliancecan.ca/en).

To determine whether the splines vary with species, we run an interaction model of covariates:

$$\begin{aligned}t_{chk} &= \sum_{i=1}^{Nc}\sum_{p=1}^{Np} s_{cpi}^{(1)}\left(\overline{clim}_{ih}\right)+\sum_{i=1}^{No}\sum_{p=1}^{Np} s_{cpi}^{(2)}\left(ontogeny_{ihk}\right)\\&+\sum_{p=1}^{Np} s_{cp}^{(3)}\left(elevation_h\right)+s_c^{(4)}(spatial)\\&+s_c^{(5)}\left(Z_hB_h\right)+\varepsilon_{chk}.\end{aligned}\tag{4}$$

In this interaction model, the fitting process optimizes the performance where some species may behave differently from others, in interactions with environmental covariates. To determine whether or not growth sensitivity patterns are considered to be best represented by this model that includes species × covariates interactions (i.e. Equations 4 vs. 3), we compared Akaike's information criterion (AIC) of the two models after re-running both using the maximum likelihood (ML) method in 'bam' function (Faraway, 2016; Zuur et al., 2009). Due to limited computing memory relocation resources, these runs were conducted using a subset of the data that included a maximum of two trees randomly selected for each species within a 1° grid. The size of this subset is around 7300 samples, which accounts for nearly one-fourth of the original dataset. It was determined by consideration of available computing resources on the Narval cluster of Compute Canada. A lower AIC score for equation 4 tells us that the interaction term improves the performance of our model.

The two sets of models formulated using Equations (3) and (4) allow the inferences of climatic sensitivity in interaction with environmental gradients over the whole country. However, since the sampling and climatic gradients of the different species in these models are unequal, the results will be influenced by those with greater representativeness. In the second step, we explored the

effects of environmental covariates on growth sensitivity by running species-specific GAMs for the 10 most widely distributed tree species:

$$t_{chkp} = \sum_{i=1}^{N_c} s_{cpi}^{(1)}(clim_{ih}) + \sum_{i=1}^{N_o} s_{cpi}^{(2)}(ontogeny_{ihk}) + s_{cp}^{(3)}(spatial) + s_{cp}^{(4)}(Z_h B_h) + \varepsilon_{chkp}. \quad (5)$$

Here, we were interested in knowing how climate sensitivity t depends smoothly on covariates, the hypothesis being that the effects of MAT and MAP are felt towards the cold and warm edges (or wet and dry edges) of the tree species' sample distributions. This hypothesis is tested by examining the confidence intervals (CIs) of the covariate's predicted fits, which here are zero-centred. The null hypothesis 'no edge effect' is rejected whenever the CIs at the extremes or limits of the range of the species' data exclude zero (see Figure S2; Simpson, 2018). All tests were two-sided, that is, we made no hypothesis about the directionality of responses. The strength and significance of covariates were determined using the associated F-ratio and p-value. We used the 'bam' function, $k=5$, and the fREML method to fit these species' models.

3 | RESULTS

3.1 | Quantification of growth sensitivity to climate

Of all tree samples analysed, 78% had a significant relationship with minimally one of the five climate predictors (FFD, $SMD_{(T-1)}$, $VPD_{(T-1)}$, $SMD_{(T)}$, $VPD_{(T)}$: Figure 2). FFD had the highest percentage of significant t statistics (39%), followed by $SMD_{(T)}$ (37%). Variables $SMD_{(T-1)}$ and $VPD_{(T-1)}$ followed with equivalent percentages (29%). Overall, relationships to FFD, SMD and VPD were somewhat more negative than positive, that is, high values in these indices were more often detrimental to growth (Figures 2a and 3a).

The distribution of t statistics was not random across the country. Moran's I spatial correlograms indicated significant spatial clustering in the observed pattern of annual growth sensitivity to FFD, SMD and VPD ($p<0.050$, Table 1). Particularly, high Moran I values were noted for $SMD_{(T)}$ and $VPD_{(T)}$ (Moran $I=0.39$ and 0.36, respectively), while $VPD_{(T-1)}$ showed the least autocorrelation (Moran $I=0.26$). In terms of spatial distribution, sensitivity to FFD was most negative in the western mountainous regions and in the central-eastern part of the country (Figure 3b). Besides, negative sensitivity to $SMD_{(T)}$ was clustered eastward of the mountainous regions (Figure 3d). One may note that much of the area showing sensitivity to $SMD_{(T)}$ lacked sensitivity to FFD (Figure 3b vs. 3d). Conversely, $SMD_{(T-1)}$ showed a clustering of negative t statistics in the southeastern sector of the mountain ranges (Figure 3c), whereas negative growth sensitivity to $VPD_{(T-1)}$ was distributed relatively more homogeneously across the country (Figure 3e). Finally, clusters of positive sensitivity to $VPD_{(T)}$ were noted in northeastern areas of the country and high elevation in the western mountainous regions (Figure 3f).

At species' level, results depicted high inter-species variability in growth sensitivity to FFD, whereas VPD and SMD responses were more often similar across species (Figure 2b–k). For instance, it can be noted that negative sensitivity to FFD dominates over positive ones in *Picea engelmannii*, *Pinus banksiana*, *Pinus contorta* and *Pseudotsuga menziesii*, while the opposite occurs in *Picea glauca*, *Larix laricina*, *Betula papyrifera* and *Populus tremuloides*. For SMD, there is an overall resemblance in distribution of significant t statistics in *Abies balsamea*, *Picea glauca*, *Picea mariana*, *Pinus banksiana*, *Pinus contorta*, *Pseudotsuga menziesii*, and to some extent, *Betula papyrifera* and *Populus tremuloides*. For all these species, above-average SMD was detrimental to growth. The exception comes from *Picea engelmannii*, which exhibited a distinct pattern dominated by positive sensitivity to $SMD_{(T-1)}$ (Figure 2c). About the same observations were made analysing $VPD_{(T-1)}$.

3.2 | Species–covariates interactions

The fitting statistics of Equations (3) and (4) suggested that growth sensitivity to FFD, SMD and VPD across Canada was best explained by model formulations that included species × covariates interactions (Table 1). Such models had systematically lower AIC and higher adjusted R^2 (from +2% for SMD to +4% for FFD) than the models limited to additive sums of smooth functions of covariates. Species × covariates models well explained the variation for tree sensitivity to FFD (adjusted $R^2=0.90$) and $SMD_{(T)}$ (adjusted $R^2=0.76$), and less so for other variables (Table 1). In terms of importance of species × covariate interactions, *Populus tremuloides* × size, *Pinus strobus* × size, *Populus balsamifera* × size, *Abies balsamea* × size and *Pinus resinosa* × size had the highest F-ratios for the distribution of t_{FFD} across the country (F-ratios >114; Figure S3). Size interactions with *Pseudotsuga menziesii*, *Pinus banksiana*, *Picea mariana*, *Populus tremuloides* and *Picea glauca* had the strongest importance in explaining distribution of $t_{SMD(T-1)}$ (F-ratios > 105) and $t_{SMD(T)}$ (F-ratios > 61) (Figure S3). Age interactions with *Populus tremuloides*, size interactions with *Populus tremuloides* and *Pinus resinosa*, and elevation interactions with *Picea engelmannii* and *Pseudotsuga menziesii* had the largest influences in explaining the spatial pattern of $t_{VPD(T-1)}$ (F-ratios > 66). Size interactions with *Picea mariana*, *Populus tremuloides*, *Pinus banksiana*, *Picea engelmannii* and *Picea glauca* were held the strongest influences in explaining $t_{VPD(T)}$. F-ratios of species × MAT and species × MAP were generally low (Figure S3).

3.3 | Factors driving variability in growth sensitivity to climate

We determined whether tree growth sensitivity to FFD, SMD and VPD differed towards cold/wet and warm/dry edges of sampled species distributions by using species-specific GAMs applied to the 10 most sampled species. The sensitivity of growth to FFD was highly predictable by GAMs in most species studied (Equation 5), with adjusted R^2 exceeding 0.80 in all but *Larix laricina* (Table 2). The lowest predictive skills were found in *Picea mariana* when analysing growth responses to $VPD_{(T-1)}$ (Table 2). Of studied covariates, tree size was the most systematic and influential predictor (high F-ratio

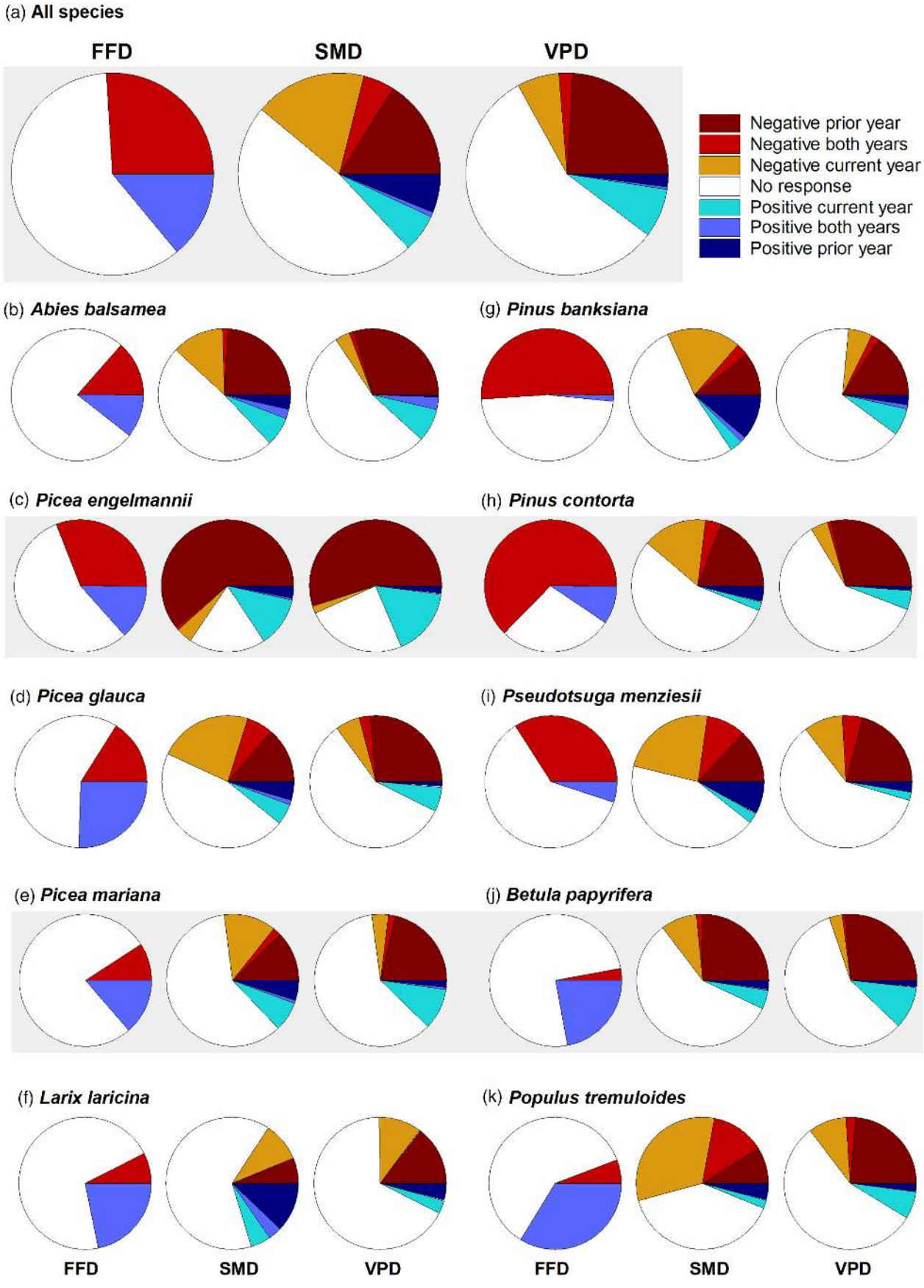

(a) All species
FFD
SMD
VPD
Negative prior year
Negative both years
Negative current year
No response
Positive current year
Positive both years
Positive prior year
(b) Abies balsamea
(c) Picea engelmannii
(d) Picea glauca
(e) Picea mariana
(f) Larix laricina
(g) Pinus banksiana
(h) Pinus contorta
(i) Pseudotsuga menziesii
(j) Betula papyrifera
(k) Populus tremuloides
FFD
SMD
VPD

FIGURE 2 Countrywide and species-specific sensitivity of radial growth to freeze and drought. Using tree-ring data from 35,784 trees across Canada, we constructed species-by-site Generalized Additive Mixed Models (GAMM) to assess the sensitivity of annual basal area increment (BAI) to cold-season freeze frequency (FFD), summer soil moisture deficit (SMD) and summer vapour pressure deficit (VPD) during 1951–2018. We included separate terms for the effects of the prior year (T–1) and current year (T) SMD and VPD on tree growth, for a total of five climate predictors (t_{FFD}, $t_{SMD(T-1)}$, $t_{VPD(T-1)}$, $t_{SMD(T)}$, $t_{VPD(T)}$: see Section 2). The t statistics obtained from GAMMs indicate the strength of the statistical associations between growth and the climate predictors. Illustrated here is the proportion of significant t-values ($p < 0.050$, positives and negatives) considering all the species studied (a) as well as for each widespread species ($n > 100$ sites, b–f). Red colour indicates samples in which high values of the specified climate variable is detrimental to tree growth (negative t-values), white denotes an absence of relation, and blue colour indicates samples in which high values favour tree growth (positive t-values). Relationships include those occurring during the year prior to (dark red and dark blue) and current to growth (orange and light blue), as well as those simultaneously occurring during both years (cyan blue and bright red).

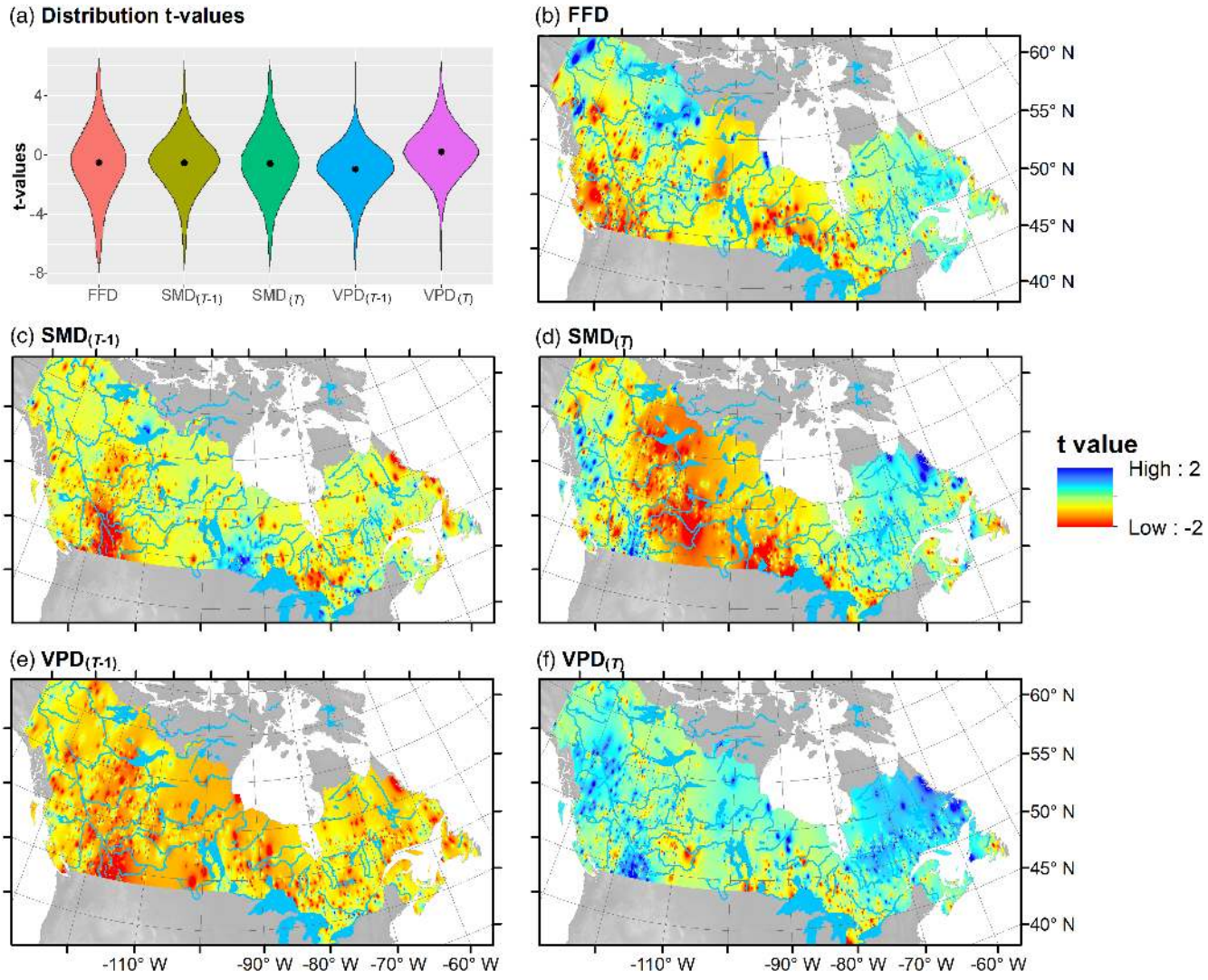


FIGURE 3 Spatial variation in tree species growth sensitivity to freeze and drought. (a) Violin plot depicting the median and the density of t-values of growth sensitivity to cold-season frequency of freeze days (FFD), summer soil moisture deficit during the current year ($SMD_{(T)}$) and prior-year growth sensitivity ($SMD_{(T-1)}$), and summer vapour pressure deficit during the current year ($VPD_{(T)}$) and the previous year ($VPD_{(T-1)}$). (b–f) Each map represents the strength of relationships between tree basal area increments (BAI, mm^2) and the illustrated factor for the period 1951–2018, expressed as t-values obtained from Generalized Additive Mixed Models (GAMMs). Negative t-values (red) indicate areas where high values of the specified variable have a negative impact on tree growth, t-values close to zero denote an absence of relation between BAI and the variable, and positive t-values (blue) indicate areas where high values favour tree growth. The maps were obtained by applying an Inverse Distance Weighted interpolation to the vector of georeferenced t-values (sampling for interpolation was set at $n = 100$ trees with a search radius of 10 degrees and resolution of 0.1 degree; ArcGIS v10.5.1).

TABLE 1 Summary statistics of generalized additive models (GAMs) relating growth sensitivity to cold-season (November–April) frequency of freeze days (FFD), summer (June–August) soil moisture deficit (SMD) and summer vapour pressure deficit (VPD), with species, ontogeny (tree size and age), local mean climatologies (mean annual temperature (MAT), mean annual precipitation totals (MAP)), elevation and random effects (spatial autocorrelation and site).

Variable	Model type	*n* trees[a]	*n* sites[a]	Obs. Moran *I* statistic	Obs. Moran *I* *p*-value	GAM adjusted R^2 (%)	Res. Moran *I* statistic	Res. Moran *I* *p*-value	GAM AIC[b]
FFD	Smooth	32,108	2658	0.333	0.000	0.859	0.026	0.145	23,837.5
FFD	Species interact	32,108	2659	0.334	0.000	0.897	0.010	0.331	23,226.9
$SMD_{(t-1)}$	Smooth	33,304	2712	0.334	0.000	0.627	0.015	0.268	25,210.9
$SMD_{(t-1)}$	Species interact	33,304	2712	0.334	0.000	0.648	−0.008	0.617	24,988.0
$SMD_{(t)}$	Smooth	33,379	2699	0.383	0.000	0.735	0.059	0.008	26,392.7
$SMD_{(t)}$	Species interact	33,379	2699	0.383	0.000	0.758	0.007	0.386	25,838.3
$VPD_{(t-1)}$	Smooth	33,349	2702	0.248	0.000	0.455	0.023	0.170	25,967.1
$VPD_{(t-1)}$	Species interact	33,349	2702	0.248	0.000	0.498	0.015	0.266	25,793.7
$VPD_{(t)}$	Smooth	33,297	2709	0.348	0.000	0.555	0.017	0.233	25,419.5
$VPD_{(t)}$	Species interact	33,297	2709	0.348	0.000	0.573	0.025	0.149	25,188.2

Note: Climate sensitivity the year prior to growth is indicated (*T*−1). Two model forms are illustrated: smooth only (Smooth) and smooth interaction with species (Species interact).

[a]Sample sizes (*n*) may differ between analyses because of rare instances of non-converging site-level generalized additive mixed models used for determining climate sensitivities.

[b]Akaike's information criterion (AIC) of the two models after re-running both using the maximum likelihood (ML) method in 'bam' function. AIC comparison is only valid for the pairs of models for the same variable. Obs., observations; Res., model residuals.

and low *p*) of growth sensitivity to FFD, $SMD_{(T-1)}$, $SMD_{(T)}$ and $VPD_{(T)}$: All tested species exhibited significant tree size effects at the 5% level, and most often with high *F*-ratios (Figure 4). Tree size contributed to raising t_{FFD}, $t_{VPD(T-1)}$ and $t_{VPD(T)}$, while lowering $t_{SMD(T-1)}$ and $t_{SMD(T)}$ (Figure 5). Age was also frequently found to be a significant predictor, with 86% of significant *p*-values (Figure 4).

The importance of climate predictors was contextual to species (Figure 4). Effects of MAT and MAP generally had low predictive power, with respectively 24% and 22% of significant *p*-values (Figure 4). Relative to their population average, four species exhibited enhanced positive sensitivity to SMD at the cold edge of their species range (Figure 6; Figures S4–S9). Two more species exhibited enhanced positive sensitivity to SMD at their wet edge; one species had both cold and wet edges responding stronger than its population range (Figure 6b). The spatial pattern of MAT influence on $t_{SMD(T)}$ was particularly well defined for *Pseudotsuga menziesii*, with a more negative growth response to $SMD_{(T)}$ predicted in coastal regions and positive ones in mountains and mountain plateaus (Figure 7f). A similar spatial pattern was observed in sensitivity of *Pinus contorta* to $SMD_{(T-1)}$, albeit this one being more related to MAP than MAT (Figures 4 and 7e). Four species also exhibited enhanced positive sensitivity to VPD at their cold edge (Figure 6a). The predicted responses of *Picea glauca*, *Picea mariana*, and to a lesser extent *Larix laricina*, were notorious, with clear gradients from below-average $t_{VPD(T)}$ in the southeast to above-average values in the northwest of the country (Figure 7). At the dry edge of sample distributions, three species exhibited enhanced negative sensitivity to either SMD or VPD (e.g. *Picea engelmanii*, *Abies balsamea* and *Betula papyrifera*; Figures 6d and 7d), whereas four species had such enhanced negative sensitivity appearing at their warm edge (e.g. *Pseudotsuga menziesii*, *Betula papyrifera*, *Picea glauca* and *Larix Laricina*; Figure 6c). *Betula papyrifera* had a rather complex sensitivity to VPD (Figure 6b,d); however, it can be broadly deduced that the species exhibited below-average $t_{VPD(T-1)}$ at its wet edge, while concurrently demonstrating increased positive $t_{VPD(T)}$ at the same edge.

Sensitivity to FFD along climate gradients was more ambiguous. MAT was a significant predictor of responses of growth to FFD in *Populus tremuloides*, *Picea engelmannii* and *Picea glauca*. The cold edge of the sampled distribution featured a more positive the sensitivity of growth to FFD in *P. glauca* than the warm one (Figure 6). In the case of *Populus tremuloides*, the pattern was reversed, meaning that the warmer edge of the sample distribution showed a more negative growth sensitivity to FFD compared with the colder edge (Figure 6). At dry edges, two species exhibited an increased positive sensitivity to FFD (*Betula papyrifera* and *Pseudotsuga menziesii*), while one species displayed an intensified negative sensitivity at its wetter edge (*Picea engelmannii*) (Figure 6).

4 | DISCUSSION

4.1 | Global picture of growth sensitivity to freeze and drought of tree species

We documented the biogeography of tree growth sensitivity to freeze days (FFD), SMD and VPD using an extensive network of

TABLE 2 Summary statistics of species-specific generalized additive models (GAMs) relating growth sensitivity to cold-season (November–April) frequency of freeze days (FFD), summer (June–August) soil moisture deficit (SMD) and summer vapour pressure deficit (VPD), with species, ontogeny (tree size and age), local mean climatologies (mean annual temperature (MAT), mean annual precipitation totals (MAP)), elevation and random effects (spatial autocorrelation and site).

Species	Variables	*n* trees[a]	*n* sites[a]	Obs. Moran *I* statistic	Obs. Moran *I* *p*-value	GAM adjusted R^2 (%)	Res. Moran *I* statistic	Res. Moran *I* *p*-value
Abies balsamea	FFD	756	183	0.108	0.123	0.870	0.029	0.360
	SMD_T	762	184	0.473	0.000	0.860	−0.049	0.669
	$SMD_{(T-1)}$	739	178	0.259	0.004	0.874	−0.196	0.971
	VPD_T	764	185	0.241	0.006	0.683	−0.185	0.967
	$VPD_{(T-1)}$	766	184	0.109	0.120	0.673	−0.055	0.693
Betula papyrifera	FFD	547	145	0.135	0.096	0.922	−0.064	0.696
	SMD_T	550	146	0.161	0.059	0.887	0.048	0.307
	$SMD_{(T-1)}$	550	147	0.058	0.267	0.867	−0.025	0.561
	VPD_T	560	149	0.318	0.001	0.624	0.055	0.281
	$VPD_{(T-1)}$	553	148	−0.041	0.622	0.653	−0.227	0.980
Larix laricina	FFD	494	157	0.100	0.150	0.751	0.018	0.406
	SMD_T	483	153	0.110	0.130	0.616	−0.294	0.997
	$SMD_{(T-1)}$	489	154	0.099	0.152	0.614	0.007	0.445
	VPD_T	504	159	0.066	0.238	0.618	−0.123	0.875
	$VPD_{(T-1)}$	504	159	0.342	0.000	0.495	−0.045	0.648
Picea engelmannii	FFD	1274	113	0.550	0.000	0.879	−0.088	0.750
	SMD_T	1446	122	0.427	0.000	0.830	0.028	0.366
	$SMD_{(T-1)}$	1446	121	0.503	0.000	0.728	0.186	0.043
	VPD_T	1444	122	0.357	0.001	0.659	0.169	0.057
	$VPD_{(T-1)}$	1442	121	0.413	0.000	0.518	0.001	0.466
Picea glauca	FFD	3983	644	0.053	0.026	0.947	0.063	0.089
	SMD_T	4691	717	0.489	0.000	0.748	0.093	0.045
	$SMD_{(T-1)}$	4695	717	0.262	0.000	0.615	0.075	0.084
	VPD_T	4662	711	0.391	0.000	0.580	0.068	0.105
	$VPD_{(T-1)}$	4692	718	0.250	0.000	0.472	0.120	0.015
Picea mariana	FFD	7684	1859	0.208	0.000	0.993	0.046	0.099
	SMD_T	7770	1875	0.322	0.000	0.780	−0.037	0.843
	$SMD_{(T-1)}$	7812	1884	0.134	0.000	0.557	−0.036	0.835
	VPD_T	7758	1877	0.340	0.000	0.403	0.046	0.099
	$VPD_{(T-1)}$	7786	1886	0.080	0.013	0.342	0.001	0.476

(Continues)

TABLE 2 (Continued)

Species	Variables	*n* trees[a]	*n* sites[a]	Obs. Moran *I* statistic	Obs. Moran *I* *p*-value	GAM adjusted R^2 (%)	Res. Moran *I* statistic	Res. Moran *I* *p*-value
Pinus banksiana	FFD	3884	638	0.300	0.000	0.880	0.044	0.232
	SMD_T	3914	649	0.340	0.000	0.583	−0.061	0.818
	$SMD_{(T-1)}$	3895	639	0.171	0.004	0.551	0.084	0.091
	VPD_T	3893	638	0.047	0.219	0.795	−0.017	0.592
	$VPD_{(T-1)}$	3863	627	0.090	0.076	0.539	−0.148	0.988
Pinus contorta	FFD	2746	254	0.297	0.000	0.913	−0.159	0.965
	SMD_T	2830	259	0.354	0.000	0.586	0.044	0.284
	$SMD_{(T-1)}$	2840	264	0.465	0.000	0.636	−0.120	0.916
	VPD_T	2831	261	0.342	0.000	0.428	−0.066	0.767
	$VPD_{(T-1)}$	2830	261	0.254	0.001	0.452	0.023	0.374
Populus tremuloides	FFD	3559	696	0.274	0.000	0.981	0.052	0.180
	SMD_T	3628	720	0.380	0.000	0.768	0.025	0.322
	$SMD_{(T-1)}$	3623	718	0.259	0.000	0.748	−0.097	0.948
	VPD_T	3620	714	0.369	0.000	0.721	−0.030	0.686
	$VPD_{(T-1)}$	3627	717	0.249	0.000	0.837	0.007	0.440
Pseudotsuga menziesii	FFD	2744	223	0.176	0.053	0.830	−0.022	0.550
	SMD_T	2818	230	0.247	0.012	0.633	−0.114	0.828
	$SMD_{(T-1)}$	2730	227	0.741	0.000	0.763	0.067	0.248
	VPD_T	2779	227	0.330	0.001	0.453	−0.050	0.647
	$VPD_{(T-1)}$	2807	228	0.534	0.000	0.611	0.112	0.142

Note: Climate sensitivity the year prior to growth is indicated (*T*−1). A Moran *I* is considered significant if $p < 0.050$. Sample depths for trees and sites are indicated.

[a]Sample sizes (*n*) may differ between analyses because of rare instances of non-converging site-level generalized additive mixed models used for determining climate sensitivities.

tree-ring data covering Canada's forests and explored some of the covariates behind the distribution of this sensitivity. The proportion of trees responding to FFD, SMD and VPD was quite equal across the country, with an overall negative impact of these variables on tree growth (Figure 2). These climate sensitivities were not randomly distributed across the country, but largely stringent to the presence of focal species in interaction with tree size. At the species level, tree growth sensitivity interacted with prevailing subcontinental climatic gradients in a few species, leading to differentiations at the cold/wet and warm/dry edges of their respective sampled distributions (Figures 6 and 7). However, evidence was found to support the notion of climate sensitivity being a random trait across space for numerous species, including widespread species of genus *Picea*, *Pinus* and *Populus*. Biogeographical predictions suggest that populations located at the limits of their ranges would be more sensitive to climatic fluctuations as conditions approach the tolerance limits of the species (Camarero et al., 2021; Matías et al., 2017). In the boreal forest, individuals of a given tree species usually grow better at warmer temperatures than at colder ones (Way & Oren, 2010). Species distribution models are based on this principle of climatically suitable

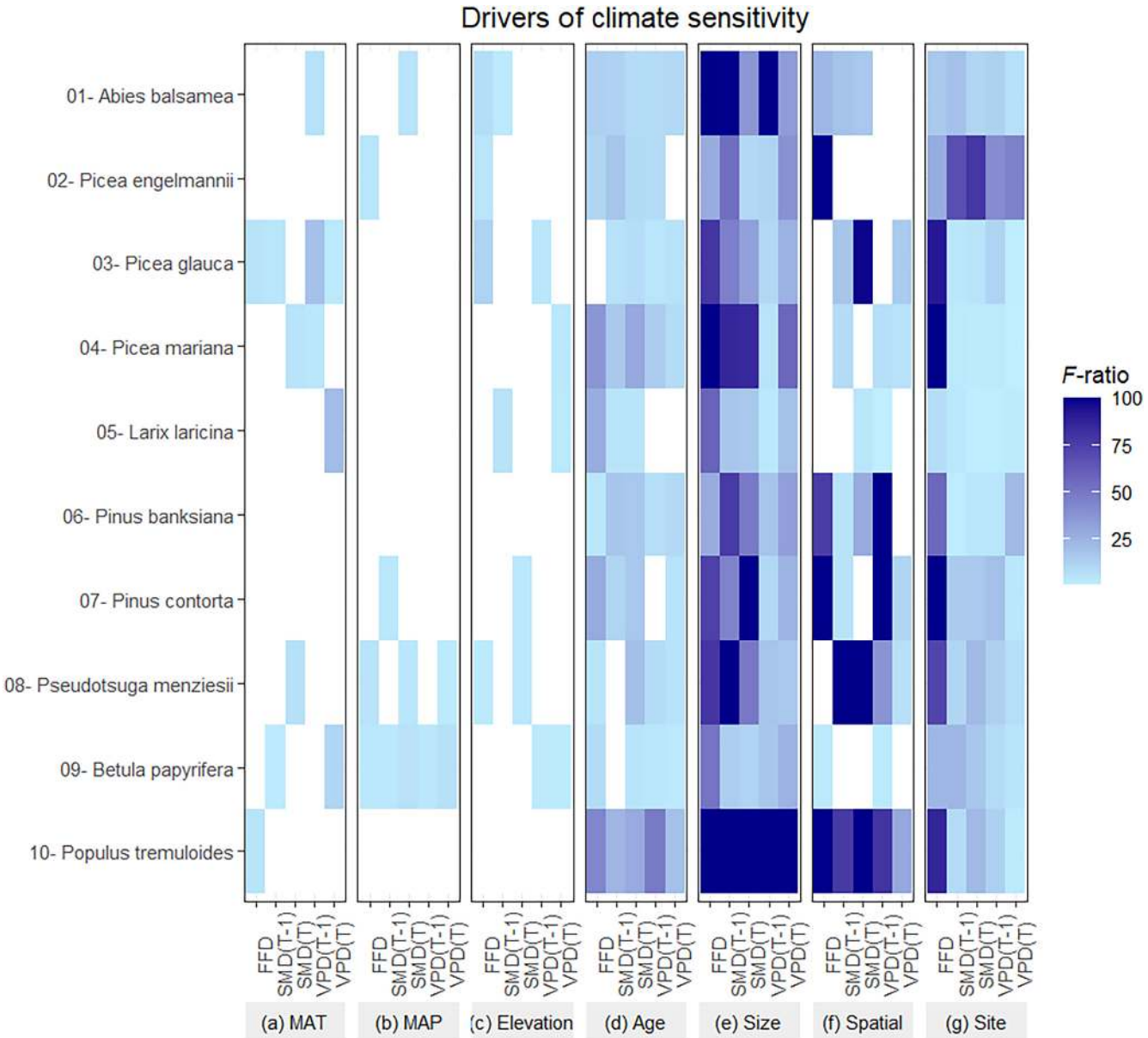


FIGURE 4 Species-species variations in growth sensitivity to climate relative to climatic, ontogenic and geographic factors. The heatmaps present the magnitude of the growth sensitivity to cold-season frequency of freeze days (FFD), summer moisture deficit (SMD) and vapour pressure deficit (VPD) relative to mean annual temperature (MAT; (a)), mean annual precipitation (MAP (b)), elevation (c), tree age (Age; (d)), tree size (Size; (e)), joint effects of latitude and longitude (Spatial; (f)), and site (Site; (g)) random effects. $SMD_{(T-1)}$ and $VPD_{(T-1)}$ are for the prior year to growth. A generalized additive model (GAM) of relationships between *t*-values and the explanatory variables generated the *F*-ratios shown here. Non-significant variables ($p > 0.050$, $F \cong 0$) were attributed white colour. Tree age is the cambial age of the outermost ring, whereas tree size is the estimated tree basal area (BA).

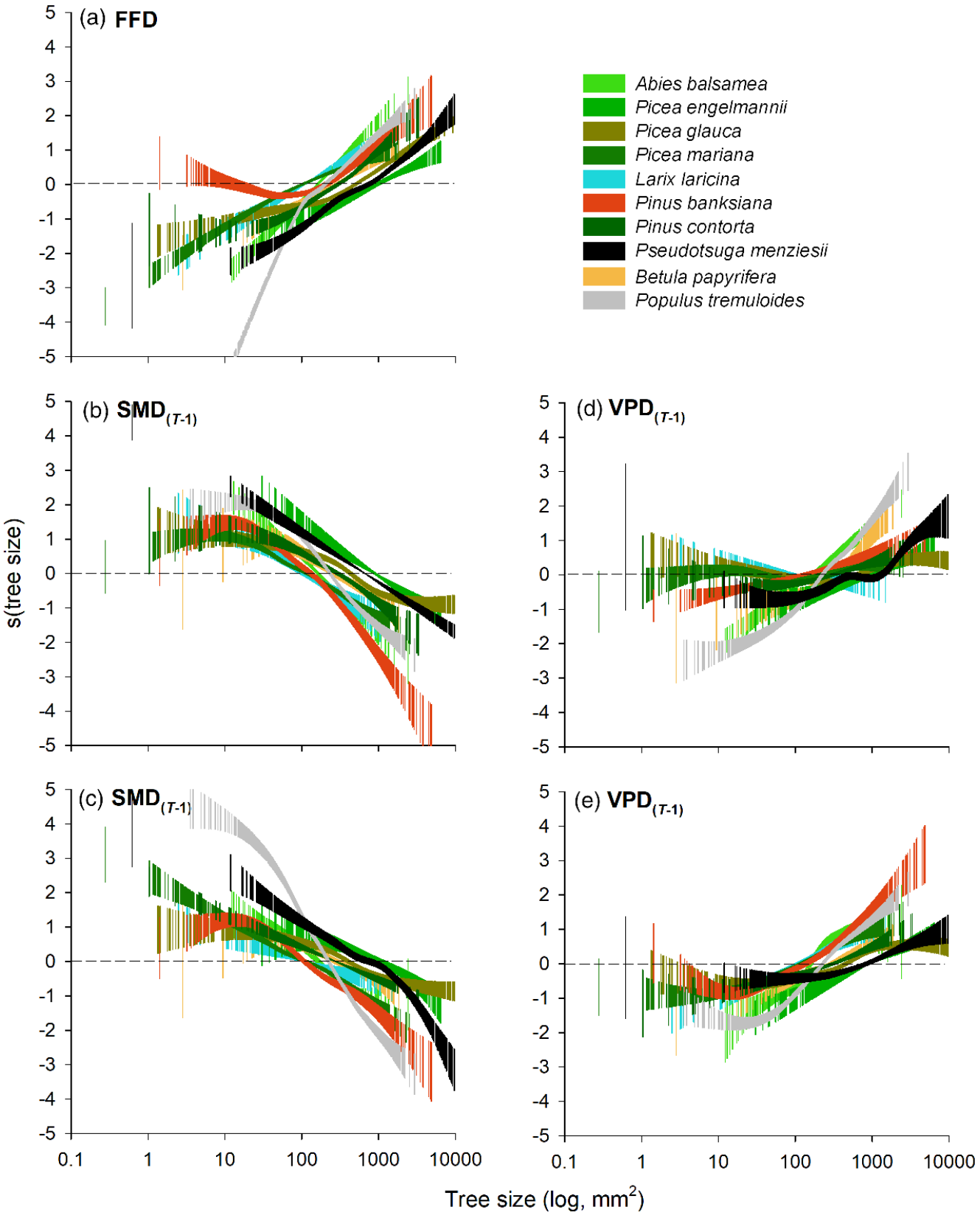


FIGURE 5 Fitted smooth functions of tree size (expressed as basal area, log-scaled) for the sensitivity *t* of growth to (a) frequency of freeze days (FFD), (b–c) summer soil moisture deficit (SMD) and (d–e) vapour pressure deficit (VPD), for 10 tree species. Effects were determined using species-specific generalized additive models (GAM) and are shown here by the 95% confidence intervals of smoothed (*s*) fits between *t* and tree size (zero-centred). Each bar represents a tree sample. The zero line defines whether tree size effects on sensitivity *t* are below or above average for a given species. The null hypothesis 'no effect of tree size on sensitivity *t*' is rejected whenever the confidence intervals exclude zero. It can be noted that the detrimental influence of $VPD_{(T-1)}$ on growth was stronger in small trees, while the detrimental influences of $SMD_{(T-1)}$ and $SMD_{(T)}$ were more strongly felt in large trees.

habitat between rear and leading edges of species distributions: they typically project considerable increases in climatically suitable habitat for tree species at northern leading edges, and declines at rear edges, with warming (Bernal-Escobar et al., 2022; Boisvert-Marsh et al., 2022; McKenney et al., 2007). Spatial projections based on static-tree growth and climate relationships corroborate these predictions, with strong temperature limitation of tree growth in cold and humid regions, and strong precipitation limitation in dry regions (Babst et al., 2019; Charney et al., 2016). Stand-level ecophysiological models of forest growth also echo these predictions (Girardin, Hogg, et al., 2016). Our results indicate that these predictions are only partially valid, so caution is warranted.

4.2 | Growth sensitivity to climate towards species range edges

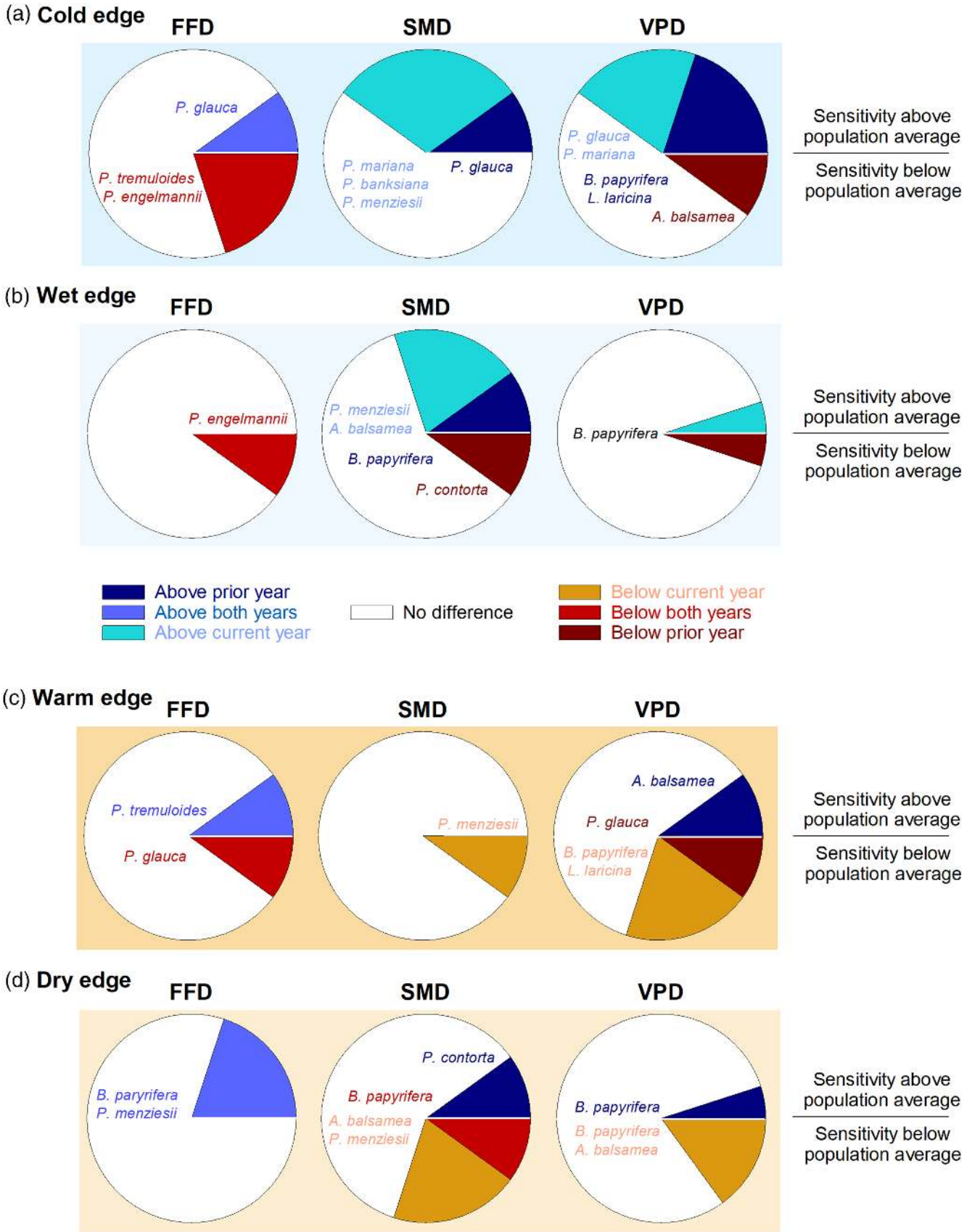
Thermal sensitivity inferred from the growth relationship to FFD in our study was not unanimous at the cold and warm edges. Rather, the most compelling indication of thermal effects was at dry edges of *Betula papyrifera* and *Pseudotsuga menzienii*. There, detrimental effects of high FFD, like freeze damage to roots, needles or leaves, were seemingly dampened in comparison to the reminder of their respective populations (Girardin et al., 2022). Nonetheless, an indirect thermal limitation on the growth occurring through the moisture conditions of the site cannot be ignored. Indeed, we find that seven of the 10 widespread species studied have an above-average *t* statistics to drought indices (VPD and/or SMD) at cold margin of sample distributions (Figure 5). In these environments, tree growth is therefore interpreted as not being particularly negatively affected by drought; on the contrary, drought below stressful conditions can help alleviate unfavourable growth conditions associated with cold environments (Mirabel et al., 2023). In northern boreal forests, low temperatures are often associated with shorter growth periods, nutrient-poor soil conditions, abundant annual snowfall, poor drainage, and late snowmelt and soil thawing, which are all factors limiting photosynthesis and delaying initiation of growth (Jarvis & Linder, 2000; Pau et al., 2022; Verbyla, 2015). This limited growing season can lead to a higher growth sensitivity to mean summer energy-related indices, as the trees have less time to accumulate resources and complete critical growth processes before winter returns (Babst et al., 2019).

Of the 10 best-replicated species, six had negative drought impacts (VPD and/or SMD) more strongly being expressed at their warm/dry edges (Figures 6 and 7). This finding is consistent with expectations of productivity being under the control of summer moisture in the warmest/driest regions (Fei et al., 2017; Girardin, Hogg, et al., 2016; Pau et al., 2022). Therein, the growing season typically extends into late spring and summer, with an abundance of sunlight and warmth during June and July (Zhang et al., 2020). In general, increased temperatures accelerate the initiation of xylem formation in boreal trees, leading to an extended growing season that enables trees to optimize their photosynthetic activity and allocate resources more effectively (Zhang et al., 2020). In addition, trees with deeper root systems will demonstrate greater efficiency in accessing subsoil water, thus lowering their susceptibility to water stress throughout the growing season (Pirtel et al., 2021). For example, *Picea engelmanni* and *Pseudotsuga menziesii* rely on these deep water sources as important reservoirs to meet their water demands (Berkelhammer et al., 2020; Martin et al., 2018). Conversely, because of relatively shallow rooting systems, tree species in boreal forests (e.g. *Picea mariana*) often have limited access to deep groundwater sources and use almost exclusively shallow soil water storage. In addition, these species close stomata more stringently compared to drought-tolerant species (e.g. *Pinus banksiana*) when atmosphere and soil conditions become increasingly dry to save water and maintain their hydraulic integrity (Marchand et al., 2021). Besides the depth of the root system, many other morphological characteristics such as root diameter, branch configuration, needle morphology or xylem architecture can also influence the timing and severity of drought stress in trees (Baldi & La Porta, 2022). From a temporal perspective, in many of the studied species, the detrimental influences of drought occurred the following year. Drought during late summer and autumn may affect the dynamics of carbohydrate reserve accumulation, thereby negatively affecting spring growth (Chuste et al., 2020). Decreased reserve formation of stressed trees can also result from accelerated respiration, which leads to higher and more rapid use of photosynthates that otherwise would be available for storage (Anderegg et al., 2013; Granda & Camarero, 2017; Sala et al., 2010).

4.3 | Drought sensitivity and tree size

A noteworthy finding was the alteration of sensitivity to VPD and SMD with tree size (Figure 5). While young trees seem to be under the control of VPD, the drought signal evolves with size towards an increase in the importance of water availability, and this would be relatively valid for most tree species under study. These findings echo previous large-scale studies reporting a more detrimental impact of water deficit on growth and mortality rates of larger trees (Bennett et al., 2015; Ryan, 2015; Stovall et al., 2019). These are generally more vulnerable to reduced soil water content because of greater exposure of crowns to atmospheric evaporative demand or greater inherent vulnerability to cavitation (Bennett et al., 2015; López et al., 2021; Trouillier et al., 2019). Ontogeny-related changes in a tree's physiological needs and in the efficiency of its hydraulic network can also modify its sensitivity to climate (Altman et al., 2017; Marchand et al., 2021).

Since our results are based on contributed data whose ring-width measurements were taken primarily on dominant and co-dominant trees (Figure S10), it is possible that the size of trees as well as their response to VPD and SMD be in part related to the suitability and quality of sites for their growth (Fu et al., 2022; Skovsgaard & Vanclay, 2013). Adverse environments imposed by low temperatures and waterlogged soil conditions can result in the



selection of traits maximizing survival at the expense of growth performances in many of the studied regions (Denneler et al., 2000; Girardin et al., 2001). A lack of phenotypic adaptations to dry/warm conditions, or low level of carbon reserves in small-sized individuals because of nutrient-poor soils (with slow decomposition) can also explain their higher vulnerability to high VPD (López et al., 2021;

FIGURE 6 Summary of species-specific generalized additive models (GAM) results for the effects of MAT and MAP at the (a) cold, (b) wet, (c) warm and (d) dry edges of the tree species' sample distributions. Pie charts illustrate the proportion of species ($N = 10$) showing significant edge effects in fitted smooth functions of growth sensitivity to cold-season (November–April) frequency of freeze days (FFD), summer (June–August) soil moisture deficit (SMD) and summer vapour pressure deficit (VPD). The colour schemes define whether effects are below or above average at cold/wet and warm/dry edges of the species' sample distributions. For example, 4 of the 10 species (i.e. 40%) show positive sensitivity to SMD at their cold edge: for three species, this relationship occurs in the current year of growth and for the other, in the year before growth. See Figures S5–S9 for the original species-specific fitted smooth functions.

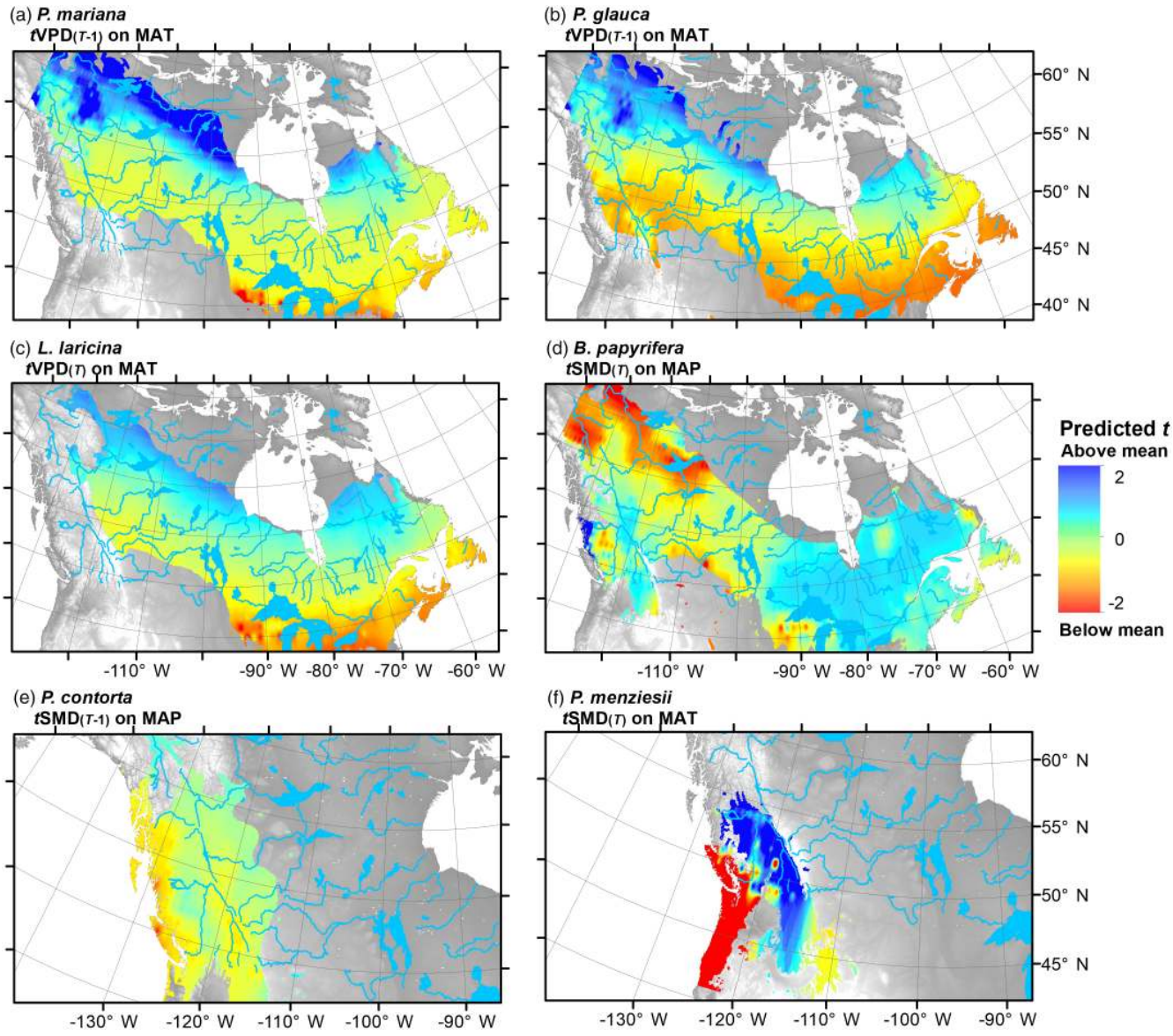


FIGURE 7 Fitted smooth functions of covariates MAT and MAP on the sensitivity *t* of growth to summer soil moisture deficit (SMD) and vapour pressure deficit (VPD) for widespread tree species. The fits were determined using generalized additive models (GAM) and are shown here after projecting on coordinate spaces and delineating using species range maps (Little, 1971). A low predicted *t* (red colour) indicates that the specified variable (SMD or VPD) is detrimental to growth, whereby a given covariate (MAT or MAP) places this response along the climate gradient. (a) Smoothed fits of growth response to $VPD_{(T-1)}$ along the MAT gradient in *Picea mariana*, (b) smoothed fits of growthresponse to $VPD_{(T-1)}$ along the MAT gradient in *Picea glauca*, (c) smoothed fits of growth response to $VPD_{(T)}$ alongthe MAT gradient in *Larix laricina*, (d) smoothed fits of growth response to $SMD_{(T)}$ along the MAP gradient in *Betulapapyrifera*, (e) smoothed fits of growth response to $SMD_{(T-1)}$ along the MAP gradient in *Pinus contorta*, and (f) smoothed fits of growth response to $SMD_{(T)}$ along the MAT gradient in *Pseudotsuga menziesii*.

Zhang et al., 2021). Notably, nitrogen fertilization has been shown to allow trees to buffer the negative effects of droughts through a better use of non-structural carbohydrates (Wang et al., 2022), which could explain our observations of a less negative response of bigger trees to VPD. These individuals also tend to be exposed to drier conditions compared with northernmost small-sized populations. The negative effects of SMD seen in larger trees may hence also reflect a combination of inadequate nutrient levels and increased water requirements. Finally, differences in climate sensitivities can also result from contrasting resource allocation strategies. This may include the ratio of allocation of root to shoot biomass, but also in carbon allocation to defence mechanisms and to reproductive structures against pests and disturbances (Stephenson et al., 2011).

4.4 | Climate sensitivity and local acclimation and adaptation

Several species examined exhibited varying levels of climate sensitivity gradients across their sampling range, ranging from moderate to none. However, when considering species with extensive ranges such as *Picea mariana*, *Picea glauca*, *Populus tremuloides* and *Pinus banksiana*, there is insufficient evidence to suggest an increased sensitivity to SMD at the warm/dry limit of their range. Only half of the studied species also showed evidence of gradients in sensitivity to FFD. In comparison, tree growth of the most common tree species in eastern United States forests showed little variation in their sensitivity to climate fluctuations across broad climatic gradients (Canham et al., 2018). Thus, our findings provide additional support to previous indications of phenotypic acclimation or local genetic adaptation in terms of growth sensitivity to the long-term mean climate. We recognize that analyses as undertaken here do not allow us to discriminate between phenotypic acclimation versus genetic adaptation. On the one hand, the lack of species-level variation in climate sensitivity may be attributed to the occupancy of microhabitats towards the edges, which fit the physiological requirements of the trees (Camarero et al., 2021). On the other hand, there is also clear evidence of widespread local adaptation in trees (Alberto et al., 2013; Leimu & Fischer, 2008). It is crucial to emphasize that adaptation is not limited solely to temporal aspects, as it includes not only the changes observed over extended generations but also extends into spatial dimensions. This is particularly evident in the presence of distinct genetic lineages spanning the entire distribution range of tree species (e.g. Girardin, Isabel, et al., 2021; Tóth et al., 2019).

According to the literature, the tree species distributed over a wide area and analysed here have significant genetic variation. For example, both local genetic adaptation and high genetic diversity have been demonstrated for drought resilience within populations of *Picea glauca*, one of the most adaptive conifer species in North America (Depardieu et al., 2020; Royer-Tardif et al., 2021). The absence of susceptibility of trees to SMD towards the dry edge is consistent with provenance trials conducted with this species, where populations from drier origins had better growth resilience to extreme drought events, compared with populations from relatively wetter origins (Depardieu et al., 2020). Analyses of climate sensitivity in provenance trial populations of *Picea mariana* also revealed the presence of local adaptation (Girardin, Isabel, et al., 2021). The strength of the positive association between increased annual biomass and winter snowfall was strongly related to seed source MAP (Girardin, Isabel, et al., 2021), which may echo the lack of a MAP gradient effect on the sensitivity of this species noted here.

In the boreal hardwood tree *Populus tremuloides*, populations diverged in cold adaptation and fall leaf phenology marking a genetic adaptation to frost (Ding & Brouard, 2022; Girardin et al., 2022). Since the colder ecological optimum for this species will not match current and future warmer climatic conditions (Ding & Brouard, 2022), the greater sensitivity of growth to cold in the warm edge compared to the cold edge may indicate a maladaptation and a potential decline of local populations in the southernmost part of the range in this species. Besides, *Pinus contorta* and *Pseudotsuga menziesii* are two widespread tree species across a range of contrasting environments in western Canada, with a genetic differentiation determined primarily by temperature variables, except for high-elevation populations more associated with high precipitation (Liepe et al., 2016). The observed negative growth response to SMD in coastal regions and positive ones in mountains and mountain plateaus for *Pinus contorta* and *Pseudotsuga menziesii* highlights the considerable heterogeneity in climate sensitivity across their range, as previously described (Griesbauer & Scott Green, 2010; McCullough et al., 2017). In the context of climate change, our observations certainly indicate a more positive impact for trees growing in cooler locations than in hot locations, where the negative effects of summer droughts may offset the positive effects of higher annual temperatures (McLane et al., 2011).

5 | CONCLUSIONS

The present work underscores the need to use broadly distributed ecological datasets to enable accurate assessment of forest response to climate change, in line with previous assessments (e.g. Babst et al., 2019; Canham et al., 2018; Chagnon et al., 2022; Klesse et al., 2020; Marchand et al., 2019). The majority of the data used in this research consists of tree-ring measurements obtained from national and provincial forest inventories, providing a more representative source compared to the commonly employed international database. We highlighted that climate sensitivity was not randomly distributed in space but was largely related to the presence of focal species. In a few species, differentiations in tree growth sensitivity were demonstrated at the cold/wet and hot/dry boundaries of their distributions. Furthermore, the variation in climate sensitivity with tree size we observed may indicate variability in acclimation of trees throughout their lifetime. These variations will certainly have a crucial role in the adaptive capacity of trees in a future climate. We recognize that our climate sensitivity analyses do not allow us to discriminate between phenotypic acclimation versus

genetic adaptation. Despite genetic local adaptation being a major determinant of the adaptive capacity of populations to climate variation, to date it has only been incorporated in about 20 studies of climate vulnerability in animals and plants (Capblancq et al., 2020), and should be incorporated into climate change vulnerability assessments (Ikeda et al., 2017). Since productivity factors can vary with stand demographics, changes in stand structure and forest composition with increasing stand disturbances will be critical to the future sensitivity of forests to climate change. Integrating genomic data across species' geographic range, along with stand demography, into future climate sensitivity analyses will allow for a more accurate assessment of climate sensitivity within ranges and will also provide a better understanding of the underlying mechanisms of species' acclimation and adaptation to climate in a climate change perspective.

AUTHOR CONTRIBUTIONS

Martin P. Girardin and Xiao Jing Guo designed the research. Martin P. Girardin and Xiao Jing Guo performed the research. Martin P. Girardin and Xiao Jing Guo analysed the data. Martin P. Girardin drafted the figures. Martin P. Girardin, Xiao Jing Guo, Claire Depardieu and William Marchand wrote the paper.

ACKNOWLEDGEMENTS

This work was made possible thanks to the financial and in-kind support provided by the Canadian Forest Service of Natural Resources Canada for project CFS-TRenD. We acknowledge all the people and agencies that were involved in tree sample collection and processing and who hence helped to create this important resource over the decades. Further financial support was provided by the NSERC (Natural Sciences and Engineering Research Council of Canada) Discovery Grant programme (RGPIN-2019-06672).

CONFLICT OF INTEREST STATEMENT

There is no competing interest.

PEER REVIEW

The peer review history for this article is available at https://www.webofscience.com/api/gateway/wos/peer-review/10.1111/1365-2745.14275.

DATA AVAILABILITY STATEMENT

The data and R scripts generated by this study have been stored on the Figshare repository: https://doi.org/10.6084/m9.figshare.24886335.v3 (Girardin, 2024), to allow reproducibility. Raw tree-ring data has been stored on the TreeSource repository (https://treesource.rncan.gc.ca/en/treerings). Access to the raw data, obtained under agreements with organizations such as Canada's NFI and provincial partners, may be restricted. Requests for accessing such data can be made to authors and with permission of the data contributors (contact names are included in the TreeSource repository). The ITRDB dataset was obtained from the NOAA Web repository (https://www.ncdc.noaa.gov/data-access/paleoclimatology-data/datasets/tree-ring).

ORCID

Martin P. Girardin https://orcid.org/0000-0003-0436-7486
William Marchand https://orcid.org/0000-0003-2114-5244
Claire Depardieu https://orcid.org/0000-0003-1340-1586

REFERENCES

Alberto, F. J., Aitken, S. N., Alía, R., González-Martínez, S. C., Hänninen, H., Kremer, A., Lefèvre, F., Lenormand, T., Yeaman, S., Whetten, R., & Savolainen, O. (2013). Potential for evolutionary responses to climate change—Evidence from tree populations. *Global Change Biology*, *19*(6), 1645–1661. https://doi.org/10.1111/gcb.12181

Altman, J., Fibich, P., Santruckova, H., Dolezal, J., Stepanek, P., Kopacek, J., Hunova, I., Oulehle, F., Tumajer, J., & Cienciala, E. (2017). Environmental factors exert strong control over the climate-growth relationships of Picea abies in Central Europe. *Science of the Total Environment*, *609*, 506–516. https://doi.org/10.1016/j.scitotenv.2017.07.134

Anderegg, W. R. L., Kane, J. M., & Anderegg, L. D. L. (2013). Consequences of widespread tree mortality triggered by drought and temperature stress. *Nature Climate Change*, *3*(1), 30–36. https://doi.org/10.1038/nclimate1635

Babst, F., Bouriaud, O., Poulter, B., Trouet, V., Girardin, M. P., & Frank, D. C. (2019). Twentieth century redistribution in climatic drivers of global tree growth. *Science Advances*, *5*(1), eaat4313. https://doi.org/10.1126/sciadv.aat4313

Bachofen, C., Perret-Gentil, A., Wohlgemuth, T., Vollenweider, P., & Moser, B. (2021). Phenotypic plasticity versus ecotypic differentiation under recurrent summer drought in two drought-tolerant pine species. *Journal of Ecology*, *109*(11), 3861–3876. https://doi.org/10.1111/1365-2745.13762

Baldi, P., & La Porta, N. (2022). Toward the genetic improvement of drought tolerance in conifers: An integrated approach. *Forests*, *13*(12), 12. https://doi.org/10.3390/f13122016

Barriopedro, D., Fischer, E. M., Luterbacher, J., Trigo, R. M., & Garcia-Herrera, R. (2011). The hot summer of 2010: Redrawing the temperature record map of Europe. *Science*, *332*(6026), 220–224. https://doi.org/10.1126/science.1201224

Bennett, A. C., McDowell, N. G., Allen, C. D., & Anderson-Teixeira, K. J. (2015). Larger trees suffer most during drought in forests worldwide. *Nature Plants*, *1*(10), 15139. https://doi.org/10.1038/nplants.2015.139

Berkelhammer, M., Still, C. J., Ritter, F., Winnick, M., Anderson, L., Carroll, R., Carbone, M., & Williams, K. H. (2020). Persistence and plasticity in conifer water-use strategies. *Journal of Geophysical Research: Biogeosciences*, *125*(2), e2018JG004845. https://doi.org/10.1029/2018JG004845

Bernal-Escobar, M., Zuleta, D., & Feeley, K. J. (2022). Changes in the climate suitability and growth rates of trees in eastern North America. *Ecography*, *2022*, e06298. https://doi.org/10.1111/ecog.06298

Bivand, R. S., & Wong, D. W. S. (2018). Comparing implementations of global and local indicators of spatial association. *Test*, *27*(3), 716–748. https://doi.org/10.1007/s11749-018-0599-x

Boisvert-Marsh, L., Pedlar, J. H., de Blois, S., Le Squin, A., Lawrence, K., McKenney, D. W., Williams, C., & Aubin, I. (2022). Migration-based simulations for Canadian trees show limited tracking of suitable climate under climate change. *Diversity and Distributions*, *28*(11), 2330–2348. https://doi.org/10.1111/ddi.13630

Brandt, J. P. (2009). The extent of the North American boreal zone. *Environmental Reviews*, *17*(1), 101–161. https://doi.org/10.1139/A09-004

Camarero, J. J., Gazol, A., Sangüesa-Barreda, G., Vergarechea, M., Alfaro-Sánchez, R., Cattaneo, N., & Vicente-Serrano, S. M. (2021). Tree growth is more limited by drought in rear-edge forests most of the times. *Forest Ecosystems*, *8*(1), 25. https://doi.org/10.1186/s40663-021-00303-1

Canham, C. D., Murphy, L., Riemann, R., McCullough, R., & Burrill, E. (2018). Local differentiation in tree growth responses to climate. *Ecosphere*, *9*(8), e02368. https://doi.org/10.1002/ecs2.2368

Capblancq, T., Fitzpatrick, M. C., Bay, R. A., Exposito-Alonso, M., & Keller, S. R. (2020). Genomic prediction of (mal)adaptation across current and future climatic landscapes. *Annual Review of Ecology, Evolution, and Systematics*, *51*(1), 245–269. https://doi.org/10.1146/annurev-ecolsys-020720-042553

Chagnon, C., Wotherspoon, A. R., & Achim, A. (2022). Deciphering the black spruce response to climate variation across eastern Canada using a meta-analysis approach. *Forest Ecology and Management*, *520*, 120375. https://doi.org/10.1016/j.foreco.2022.120375

Charney, N. D., Babst, F., Poulter, B., Record, S., Trouet, V. M., Frank, D., Enquist, B. J., & Evans, M. E. K. (2016). Observed forest sensitivity to climate implies large changes in 21st century North American forest growth. *Ecology Letters*, *19*(9), 1119–1128. https://doi.org/10.1111/ele.12650

Chuste, P.-A., Maillard, P., Bréda, N., Levillain, J., Thirion, E., Wortemann, R., & Massonnet, C. (2020). Sacrificing growth and maintaining a dynamic carbohydrate storage are key processes for promoting beech survival under prolonged drought conditions. *Trees*, *34*(2), 381–394. https://doi.org/10.1007/s00468-019-01923-5

Cullen, R. M., & Marshall, S. J. (2011). Mesoscale temperature patterns in the Rocky Mountains and foothills region of southern Alberta. *Atmosphere-Ocean*, *49*(3), 189–205. https://doi.org/10.1080/07055900.2011.592130

Denneler, B., Bergeron, Y., & Bégin, Y. (2000). An attempt to explain the distribution of the tree species composing the riparian forests of Lake Duparquet, southern boreal region of Quebec, Canada. *Canadian Journal of Botany*, *77*(12), 1689–1698.

Depardieu, C., Girardin, M. P., Nadeau, S., Lenz, P., Bousquet, J., & Isabel, N. (2020). Adaptive genetic variation to drought in a widely distributed conifer suggests a potential for increasing forest resilience in a drying climate. *New Phytologist*, *227*(2), 427–439. https://doi.org/10.1111/nph.16551

Ding, C., & Brouard, J. S. (2022). Assisted migration is plausible for a boreal tree species under climate change: A quantitative and population genetics study of trembling aspen (*Populus tremuloides* Michx.) in western Canada. *Ecology and Evolution*, *12*(10), e9384. https://doi.org/10.1002/ece3.9384

Dyke, A. (2005). Late quaternary vegetation history of northern North America based on pollen, macrofossil, and faunal remains. *Géographie Physique et Quaternaire*, *59*(2–3), 211–262. https://doi.org/10.7202/014755ar

Eichenlaub, V. L. (1987). Lakes, effects on climate. In *Climatology* (pp. 534–539). Springer US. https://doi.org/10.1007/0-387-30749-4_103

Environment Canada. (2013). National climate data and information archive. http://climate.weatheroffice.gc.ca/

Esperon-Rodriguez, M., Rymer, P. D., Power, S. A., Challis, A., Marchin, R. M., & Tjoelker, M. G. (2020). Functional adaptations and trait plasticity of urban trees along a climatic gradient. *Urban Forestry & Urban Greening*, *54*, 126771. https://doi.org/10.1016/j.ufug.2020.126771

Evans, M. E. K., DeRose, R. J., Klesse, S., Girardin, M. P., Heilman, K. A., Alexander, M. R., Arsenault, A., Babst, F., Bouchard, M., Cahoon, S. M. P., Campbell, E. M., Dietze, M., Duchesne, L., Frank, D. C., Giebink, C. L., Gómez-Guerrero, A., García, G. G., Hogg, E. H., Metsaranta, J., … GaytÁn, S. A. V. (2022). Adding tree rings to North America's national forest inventories: An essential tool to guide drawdown of atmospheric CO_2. *BioScience*, *72*(3), 233–246. https://doi.org/10.1093/biosci/biab119

Faraway, J. J. (2016). *Generalized linear, mixed effects and nonparametric regression models* (2nd ed.). Chapman and Hall/CRC. https://doi.org/10.1201/9781315382722

Fei, S., Desprez, J. M., Potter, K. M., Jo, I., Knott, J. A., & Oswalt, C. M. (2017). Divergence of species responses to climate change. *Science Advances*, *3*(5), e1603055. https://doi.org/10.1126/sciadv.1603055

Fu, Z., Ciais, P., Prentice, I. C., Gentine, P., Makowski, D., Bastos, A., Luo, X., Green, J. K., Stoy, P. C., Yang, H., & Hajima, T. (2022). Atmospheric dryness reduces photosynthesis along a large range of soil water deficits. *Nature Communications*, *13*(1), 1. https://doi.org/10.1038/s41467-022-28652-7

Gantois, J. (2022). New tree-level temperature response curves document sensitivity of tree growth to high temperatures across a US-wide climatic gradient. *Global Change Biology*, *28*(20), 6002–6020. https://doi.org/10.1111/gcb.16313

Girardin, M. P. (2024). Effects of environmental covariates on growth sensitivity. *figshare. Dataset*. https://doi.org/10.6084/m9.figshare.24886335.v3

Girardin, M. P., Bouriaud, O., Hogg, E. H., Kurz, W., Zimmermann, N. E., Metsaranta, J. M., de Jong, R., Frank, D. C., Esper, J., Büntgen, U., Guo, X. J., & Bhatti, J. (2016). No growth stimulation of Canada's boreal forest under half-century of combined warming and CO_2 fertilization. *Proceedings of the National Academy of Sciences of the United States of America*, *113*(52), E8406–E8414. https://doi.org/10.1073/pnas.1610156113

Girardin, M. P., Guo, X. J., Gervais, D., Metsaranta, J., Campbell, E. M., Arsenault, A., Isaac-Renton, M., & Hogg, E. H. (2022). Cold-season freeze frequency is a pervasive driver of subcontinental forest growth. *Proceedings of the National Academy of Sciences of the United States of America*, *119*(18), e2117464119. https://doi.org/10.1073/pnas.2117464119

Girardin, M. P., Guo, X. J., Metsaranta, J., Gervais, D., Campbell, E., Arsenault, A., Isaac-Renton, M., Harvey, J. E., Bhatti, J., & Hogg, E. H. (2021). A national tree-ring data repository for Canadian forests (CFS-TRenD): Structure, synthesis, and applications. *Environmental Reviews*, *29*(2), 225–241. https://doi.org/10.1139/er-2020-0099

Girardin, M. P., Hogg, E. H., Bernier, P. Y., Kurz, W. A., Guo, X. J., & Cyr, G. (2016). Negative impacts of high temperatures on growth of black spruce forests intensify with the anticipated climate warming. *Global Change Biology*, *22*(2), 627–643. https://doi.org/10.1111/gcb.13072

Girardin, M. P., Isabel, N., Guo, X. J., Lamothe, M., Duchesne, I., & Lenz, P. (2021). Annual aboveground carbon uptake enhancements from assisted gene flow in boreal black spruce forests are not long-lasting. *Nature Communications*, *12*(1), 1169. https://doi.org/10.1038/s41467-021-21222-3

Girardin, M. P., Tardif, J., & Bergeron, Y. (2001). Gradient analysis of *Larix laricina* dominated wetlands in Canada's southeastern boreal forest. *Canadian Journal of Botany*, *79*(4), 444–456.

Granda, E., & Camarero, J. J. (2017). Drought reduces growth and stimulates sugar accumulation: New evidence of environmentally driven non-structural carbohydrate use. *Tree Physiology*, *37*(8), 997–1000. https://doi.org/10.1093/treephys/tpx097

Griesbauer, H. P., & Scott Green, D. (2010). Assessing the climatic sensitivity of Douglas-fir at its northern range margins in British Columbia, Canada. *Trees*, *24*(2), 375–389. https://doi.org/10.1007/s00468-009-0407-z

Guo, X., Klisz, M., Puchałka, R., Silvestro, R., Faubert, P., Belien, E., Huang, J., & Rossi, S. (2022). Common-garden experiment reveals clinal trends of bud phenology in black spruce populations from a latitudinal gradient in the boreal forest. *Journal of Ecology*, *110*(5), 1043–1053. https://doi.org/10.1111/1365-2745.13582

Hammond, W. M., Williams, A. P., Abatzoglou, J. T., Adams, H. D., Klein, T., López, R., Sáenz-Romero, C., Hartmann, H., Breshears, D. D., & Allen, C. D. (2022). Global field observations of tree die-off reveal hotter-drought fingerprint for Earth's forests. *Nature Communications*, *13*(1), 1. https://doi.org/10.1038/s41467-022-29289-2

Herrero, A., Rigling, A., & Zamora, R. (2013). Varying climate sensitivity at the dry distribution edge of *Pinus sylvestris* and *P. nigra*. *Forest*

Ecology and Management, *308*, 50–61. https://doi.org/10.1016/j.foreco.2013.07.034

Hicke, J. A., Lucatello, S., Mortsch, L. D., Dawson, J., Domínguez Aguilar, M., Enquist, O. A. F., & Gilmore, E. A. (2022). North America. In H.-O. Pörtner, D. C. Roberts, M. Tignor, E. S. Poloczanska, K. Mintenbeck, A. Alegría, M. Craig, S. Langsdorf, S. Löschke, V. Möller, A. Okem, & B. Rama (Eds.), *Climate change 2022: Impacts, adaptation, and vulnerability. Contribution of Working Group II to the Sixth Assessment Report of the Intergovernmental Panel on Climate Change* (pp. 1929–2042). Cambridge University Press. https://doi.org/10.1017/9781009325844.016

Hogg, E. H., Barr, A. G., & Black, T. A. (2013). A simple soil moisture index for representing multi-year drought impacts on aspen productivity in the western Canadian interior. *Agricultural and Forest Meteorology*, *178–179*, 173–182. https://doi.org/10.1016/j.agrformet.2013.04.025

Housset, J. M., Nadeau, S., Isabel, N., Depardieu, C., Duchesne, I., Lenz, P., & Girardin, M. P. (2018). Tree rings provide a new class of phenotypes for genetic associations that foster insights into adaptation of conifers to climate change. *New Phytologist*, *218*(2), 630–645. https://doi.org/10.1111/nph.14968

Ikeda, D. H., Max, T. L., Allan, G. J., Lau, M. K., Shuster, S. M., & Whitham, T. G. (2017). Genetically informed ecological niche models improve climate change predictions. *Global Change Biology*, *23*(1), 164–176. https://doi.org/10.1111/gcb.13470

Jarvis, P., & Linder, S. (2000). Constraints to growth of boreal forests. *Nature*, *405*, 904–905. https://doi.org/10.1038/35016154

Kawecki, T. J., & Ebert, D. (2004). Conceptual issues in local adaptation. *Ecology Letters*, *7*(12), 1225–1241. https://doi.org/10.1111/j.1461-0248.2004.00684.x

Klesse, S., DeRose, R. J., Babst, F., Black, B. A., Anderegg, L. D. L., Axelson, J., Ettinger, A., Griesbauer, H., Guiterman, C. H., Harley, G., Harvey, J. E., Lo, Y.-H., Lynch, A. M., O'Connor, C., Restaino, C., Sauchyn, D., Shaw, J. D., Smith, D. J., Wood, L., … Evans, M. E. K. (2020). Continental-scale tree-ring-based projection of Douglas-fir growth: Testing the limits of space-for-time substitution. *Global Change Biology*, *26*(9), 5146–5163. https://doi.org/10.1111/gcb.15170

Leimu, R., & Fischer, M. (2008). A meta-analysis of local adaptation in plants. *PLoS ONE*, *3*(12), e4010. https://doi.org/10.1371/journal.pone.0004010

Leites, L. P., Rehfeldt, G. E., & Steiner, K. C. (2019). Adaptation to climate in five eastern North America broadleaf deciduous species: Growth clines and evidence of the growth-cold tolerance trade-off. *Perspectives in Plant Ecology, Evolution and Systematics*, *37*, 64–72. https://doi.org/10.1016/j.ppees.2019.02.002

Liepe, K. J., Hamann, A., Smets, P., Fitzpatrick, C. R., & Aitken, S. N. (2016). Adaptation of lodgepole pine and interior spruce to climate: Implications for reforestation in a warming world. *Evolutionary Applications*, *9*(2), 409–419. https://doi.org/10.1111/eva.12345

Little, E. L. (1971). *Atlas of United States trees. Volume 1, Conifers and important hardwoods*. U.S. Dept. of Agriculture, Forest Service.

López, J., Way, D. A., & Sadok, W. (2021). Systemic effects of rising atmospheric vapor pressure deficit on plant physiology and productivity. *Global Change Biology*, *27*(9), 1704–1720. https://doi.org/10.1111/gcb.15548

Marchand, W., Girardin, M. P., Gauthier, S., Hartmann, H., Bouriaud, O., Babst, F., & Bergeron, Y. (2018). Untangling methodological and scale considerations in growth and productivity trend estimates of Canada's forests. *Environmental Research Letters*, *13*(9), 093001. https://doi.org/10.1088/1748-9326/aad82a

Marchand, W., Girardin, M. P., Hartmann, H., Gauthier, S., & Bergeron, Y. (2019). Taxonomy, together with ontogeny and growing conditions, drives needleleaf species' sensitivity to climate in boreal North America. *Global Change Biology*, *25*(8), 2793–2809. https://doi.org/10.1111/gcb.14665

Marchand, W., Girardin, M. P., Hartmann, H., Lévesque, M., Gauthier, S., & Bergeron, Y. (2021). Contrasting life-history traits of black spruce and jack pine influence their physiological response to drought and growth recovery in northeastern boreal Canada. *Science of the Total Environment*, *794*, 148514. https://doi.org/10.1016/j.scitotenv.2021.148514

Martin, J., Looker, N., Hoylman, Z., Jencso, K., & Hu, J. (2018). Differential use of winter precipitation by upper and lower elevation Douglas fir in the northern Rockies. *Global Change Biology*, *24*(12), 5607–5621. https://doi.org/10.1111/gcb.14435

Matías, L., González-Díaz, P., & Jump, A. S. (2014). Larger investment in roots in southern range-edge populations of Scots pine is associated with increased growth and seedling resistance to extreme drought in response to simulated climate change. *Environmental and Experimental Botany*, *105*, 32–38. https://doi.org/10.1016/j.envexpbot.2014.04.003

Matías, L., Linares, J. C., Sánchez-Miranda, Á., & Jump, A. S. (2017). Contrasting growth forecasts across the geographical range of Scots pine due to altitudinal and latitudinal differences in climatic sensitivity. *Global Change Biology*, *23*(10), 4106–4116. https://doi.org/10.1111/gcb.13627

McCullough, I. M., Davis, F. W., & Williams, A. P. (2017). A range of possibilities: Assessing geographic variation in climate sensitivity of ponderosa pine using tree rings. *Forest Ecology and Management*, *402*, 223–233. https://doi.org/10.1016/j.foreco.2017.07.025

McKenney, D. W., Pedlar, J. H., Lawrence, K., Campbell, K., & Hutchinson, M. F. (2007). Potential impacts of climate change on the distribution of North American trees. *BioScience*, *57*(11), 939–948. https://doi.org/10.1641/B571106

McKenney, D. W., Pedlar, J. H., Lawrence, K., Papadopol, P., Campbell, K., & Hutchinson, M. F. (2014). Change and evolution in the plant hardiness zones of Canada. *BioScience*, *64*(4), 341–350. https://doi.org/10.1093/biosci/biu016

McLane, S. C., Daniels, L. D., & Aitken, S. N. (2011). Climate impacts on lodgepole pine (*Pinus contorta*) radial growth in a provenance experiment. *Forest Ecology and Management*, *262*(2), 115–123. https://doi.org/10.1016/j.foreco.2011.03.007

Mirabel, A., Girardin, M. P., Metsaranta, J., Way, D., & Reich, P. B. (2023). Increasing atmospheric dryness reduces boreal forest tree growth. *Nature Communications*, *14*(1). https://doi.org/10.1038/s41467-023-42466-1

Pau, M., Gauthier, S., Chavardès, R. D., Girardin, M. P., Marchand, W., & Bergeron, Y. (2022). Site index as a predictor of the effect of climate warming on boreal tree growth. *Global Change Biology*, *28*(5), 1903–1918. https://doi.org/10.1111/gcb.16030

Pirtel, N. L., Hubbard, R. M., Bradford, J. B., Kolb, T. E., Litvak, M. E., Abella, S. R., Porter, S. L., & Petrie, M. D. (2021). The aboveground and belowground growth characteristics of juvenile conifers in the southwestern United States. *Ecosphere*, *12*(11), e03839. https://doi.org/10.1002/ecs2.3839

Prairie Climate Centre. (2019). *Climate change in Canada*. Climate Atlas of Canada. https://climateatlas.ca/home-page

Price, D. T., Alfaro, R. I., Brown, K. J., Flannigan, M. D., Fleming, R. A., Hogg, E. H., Girardin, M. P., Lakusta, T., Johnston, M., McKenney, D. W., Pedlar, J. H., Stratton, T., Sturrock, R. N., Thompson, I. D., Trofymow, J. A., & Venier, L. A. (2013). Anticipating the consequences of climate change for Canada's boreal forest ecosystems. *Environmental Reviews*, *21*(4), 322–365. https://doi.org/10.1139/er-2013-0042

R Development Core Team. (2022). *R: A language and environment for statistical computing*. R Foundation for Statistical Computing.

Regniere, J., & Bolstad, P. (1994). Statistical simulation of daily air temperature patterns in eastern North America to forecast seasonal events in insect pest management. *Environmental Entomology*, *23*, 1368–1380. https://doi.org/10.1093/ee/23.6.1368

Reich, P. B., Sendall, K. M., Stefanski, A., Wei, X., Rich, R. L., & Montgomery, R. A. (2016). Boreal and temperate trees show strong acclimation of respiration to warming. *Nature*, *531*(7596), 633–636. https://doi.org/10.1038/nature17142

Reiss, P. T., & Ogden, R. T. (2009). Smoothing parameter selection for a class of semiparametric linear models. *Journal of the Royal Statistical Society, Series B: Statistical Methodology*, *71*(2), 505–523. https://doi.org/10.1111/j.1467-9868.2008.00695.x

Richardson, A. D., Carbone, M. S., Keenan, T. F., Czimczik, C. I., Hollinger, D. Y., Murakami, P., Schaberg, P. G., & Xu, X. (2013). Seasonal dynamics and age of stemwood nonstructural carbohydrates in temperate forest trees. *New Phytologist*, *197*(3), 850–861. https://doi.org/10.1111/nph.12042

Royer-Tardif, S., Boisvert-Marsh, L., Godbout, J., Isabel, N., & Aubin, I. (2021). Finding common ground: Toward comparable indicators of adaptive capacity of tree species to a changing climate. *Ecology and Evolution*, *11*(19), 13081–13100. https://doi.org/10.1002/ece3.8024

Ryan, M. G. (2015). Tree mortality: Large trees losing out to drought. *Nature Plants*, *1*(10), 1–3. https://doi.org/10.1038/nplants.2015.150

Sala, A., Piper, F., & Hoch, G. (2010). Physiological mechanisms of drought-induced tree mortality are far from being resolved: Letters. *New Phytologist*, *186*(2), 274–281. https://doi.org/10.1111/j.1469-8137.2009.03167.x

Serra-Maluquer, X., Gazol, A., Anderegg, W. R. L., Martínez-Vilalta, J., Mencuccini, M., & Camarero, J. J. (2022). Wood density and hydraulic traits influence species' growth response to drought across biomes. *Global Change Biology*, *28*(12), 3871–3882. https://doi.org/10.1111/gcb.16123

Simpson, G. L. (2018). Modelling palaeoecological time series using generalised additive models. *Frontiers in Ecology and Evolution*, *6*(6), 149. https://doi.org/10.3389/fevo.2018.00149

Skovsgaard, J. P., & Vanclay, J. K. (2013). Forest site productivity: A review of spatial and temporal variability in natural site conditions. *Forestry: An International Journal of Forest Research*, *86*(3), 305–315. https://doi.org/10.1093/forestry/cpt010

Smith, N. G., & Dukes, J. S. (2013). Plant respiration and photosynthesis in global-scale models: Incorporating acclimation to temperature and CO_2. *Global Change Biology*, *19*(1), 45–63. https://doi.org/10.1111/j.1365-2486.2012.02797.x

Stephenson, N. L., van Mantgem, P. J., Bunn, A. G., Bruner, H., Harmon, M. E., O'Connell, K. B., Urban, D. L., & Franklin, J. F. (2011). Causes and implications of the correlation between forest productivity and tree mortality rates. *Ecological Monographs*, *81*(4), 527–555. https://doi.org/10.1890/10-1077.1

Stovall, A. E. L., Shugart, H., & Yang, X. (2019). Tree height explains mortality risk during an intense drought. *Nature Communications*, *10*(1), 1. https://doi.org/10.1038/s41467-019-12380-6

Tóth, E. G., Tremblay, F., Housset, J. M., Bergeron, Y., & Carcaillet, C. (2019). Geographic isolation and climatic variability contribute to genetic differentiation in fragmented populations of the long-lived subalpine conifer *Pinus cembra* L. in the western Alps. *BMC Evolutionary Biology*, *19*(1), 190. https://doi.org/10.1186/s12862-019-1510-4

Trouillier, M., van der Maaten-Theunissen, M., Scharnweber, T., Würth, D., Burger, A., Schnittler, M., & Wilmking, M. (2019). Size matters—A comparison of three methods to assess age- and size-dependent climate sensitivity of trees. *Trees*, *33*(1), 183–192. https://doi.org/10.1007/s00468-018-1767-z

Verbyla, D. (2015). Remote sensing of interannual boreal forest NDVI in relation to climatic conditions in interior Alaska. *Environmental Research Letters*, *10*(12), 125016. https://doi.org/10.1088/1748-9326/10/12/125016

Vilà-Cabrera, A., Premoli, A. C., & Jump, A. S. (2019). Refining predictions of population decline at species' rear edges. *Global Change Biology*, *25*(5), 1549–1560. https://doi.org/10.1111/gcb.14597

Wang, W., Wang, S., Hoch, G., Wang, Y., Gao, G., Gu, J., & Xu, H. (2022). Whole-tree response of non-structural carbohydrates, carbon and nitrogen concentrations in two temperate tree species to 10-year nitrogen fertilization. *Forests*, *13*(2), Article 2. https://doi.org/10.3390/f13020302

Way, D. A., & Oren, R. (2010). Differential responses to changes in growth temperature between trees from different functional groups and biomes: A review and synthesis of data. *Tree Physiology*, *30*(6), 669–688. https://doi.org/10.1093/treephys/tpq015

Wood, S. N. (2003). Thin plate regression splines. *Journal of the Royal Statistical Society, Series B: Statistical Methodology*, *65*(1), 95–114. https://doi.org/10.1111/1467-9868.00374

Wood, S. N. (2011). Fast stable restricted maximum likelihood and marginal likelihood estimation of semiparametric generalized linear models. *Journal of the Royal Statistical Society, Series B: Statistical Methodology*, *73*(1), 3–36. https://doi.org/10.1111/j.1467-9868.2010.00749.x

Wood, S. N. (2017). *Generalized additive models: An introduction with R* (2nd ed.). Chapman and Hall/CRC. https://doi.org/10.1201/9781315370279

Zhang, H., Li, X., Guan, D., Wang, A., Yuan, F., & Wu, J. (2021). Nitrogen nutrition addition mitigated drought stress by improving carbon exchange and reserves among two temperate trees. *Agricultural and Forest Meteorology*, *311*, 108693. https://doi.org/10.1016/j.agrformet.2021.108693

Zhang, S., Belien, E., Ren, H., Rossi, S., & Huang, J.-G. (2020). Wood anatomy of boreal species in a warming world: A review. *iForest*, *13*, 130–138. https://doi.org/10.3832/ifor3230-013

Zuur, A. F., Ieno, E. N., Walker, N., Saveliev, A. A., & Smith, G. M. (2009). *Mixed effects models and extensions in ecology with R*. Springer. https://doi.org/10.1007/978-0-387-87458-6

SUPPORTING INFORMATION

Additional supporting information can be found online in the Supporting Information section at the end of this article.

Figure S1: Distribution of weather stations across Canada-USA included in BioSIM software and covering in full or partly the period of 1950 to 2018.

Figure S2: Interpreting the influence of the mean annual temperature (MAT) gradient on the tree sensitivity to seasonal climate variability.

Figure S3: Heatmaps showing species-specific variations in the magnitude of the growth sensitivity to cold-season frequency of freeze days (FFD), summer moisture deficit (SMD) and vapour pressure deficit (VPD) relative to the following interacting explanatory variables: tree age, tree size, mean annual temperature (MAT), mean annual precipitation (MAP), elevation, joint effects of latitude and longitude (Spatial) and site random effects. $SMD_{(T-1)}$ and $VPD_{(T-1)}$ are for the prior year to growth.

Figure S4: Summary of species-specific generalized additive models (GAM) results for the effects of MAT and MAP at the cold and warm edges (or wet and dry edges) of the tree species' sample distributions.

Figure S5: Isolated effects of covariate on the sensitivity *t* of growth to FFD(T) for widespread tree species. Effects were determined using generalized additive models (GAM) and are shown here by the 95% confidence intervals of smoothed (*s*) fits (zero-centred).

Figure S6: Isolated effects of covariate on the sensitivity *t* of growth to SMD(T-1) for widespread tree species.

Figure S7: Isolated effects of covariate on the sensitivity *t* of growth to SMD(T) for widespread tree species.

Figure S8: Isolated effects of covariate on the sensitivity *t* of growth to VPD(T-1) for widespread tree species.

Journal of Ecology BRITISH ECOLOGICAL SOCIETY

Figure S9: Isolated effects of covariate on the sensitivity *t* of growth to VPD(T) for widespread tree species.

Figure S10: Kernel density plots illustrating the distributions of tree samples by diameter at breast height (DBH) for the entire studied species (a), as well as individual species such as *Picea mariana* (b), *Picea glauca* (c), *Pinus banksiana* (d), *Populus tremuloides* (e), *Pinus contorta* (f), *Pseudotsuga menziesii* (g), *Picea engelmannii* (h), *Abies balsamea* (i), *Betula papyrifera* (j) *Larix laricina* (k).

How to cite this article: Girardin, M. P., Guo, X. J., Marchand, W., & Depardieu, C. (2024). Unravelling the biogeographic determinants of tree growth sensitivity to freeze and drought in Canada's forests. *Journal of Ecology*, *112*, 848–869. https://doi.org/10.1111/1365-2745.14275